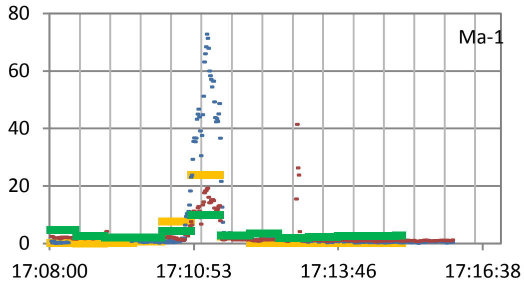
Ma-1
80
60
40
20
0
17:08:00
17:10:53
17:13:46
17:16:38

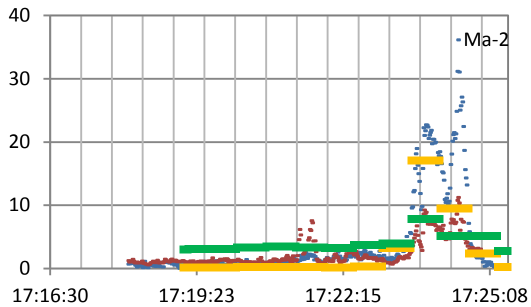
Ma-2
40
30
20
10
0
17:16:30
17:19:23
17:22:15
17:25:08

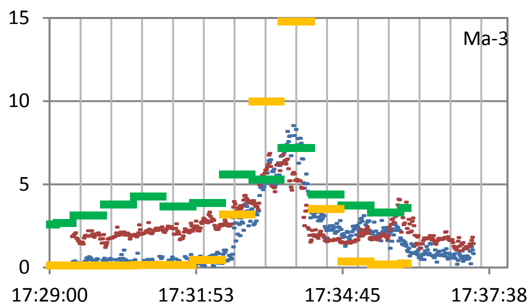
Ma-3
15
10
5
0
17:29:00
17:31:53
17:34:45
17:37:38

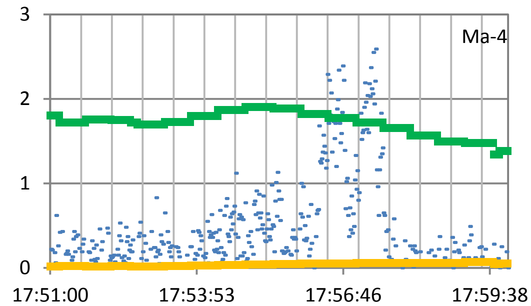
Ma-4
3
2
1
0
17:51:00
17:53:53
17:56:46
17:59:38

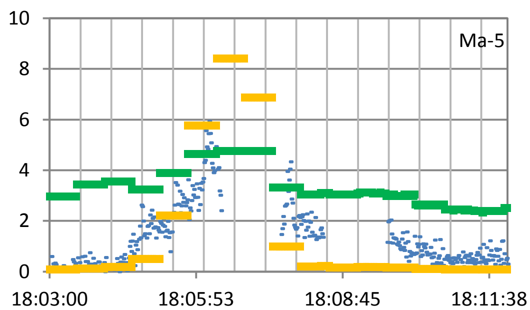
Ma-5
10
8
6
4
2
0
18:03:00
18:05:53
18:08:45
18:11:38

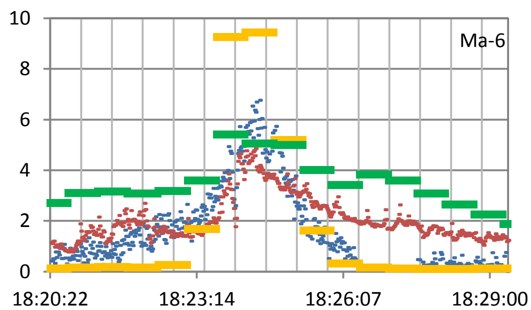
Ma-6
10
8
6
4
2
0
18:20:22
18:23:14
18:26:07
18:29:00

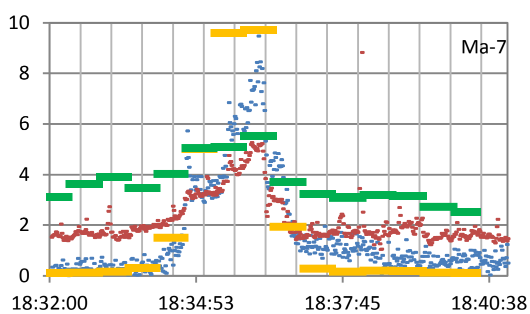
Ma-7
10
8
6
4
2
0
18:32:00
18:34:53
18:37:45
18:40:38

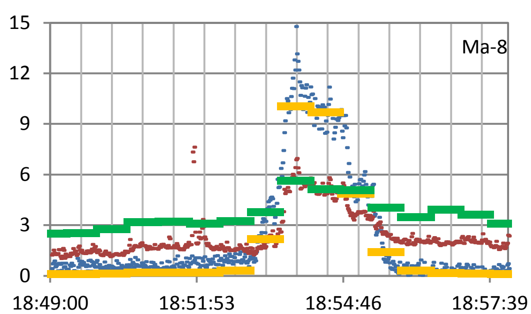
Ma-8
15
12
9
6
3
0
18:49:00
18:51:53
18:54:46
18:57:39

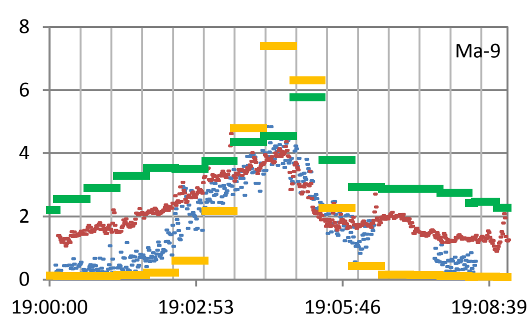
Ma-9
8
6
4
2
0
19:00:00
19:02:53
19:05:46
19:08:39

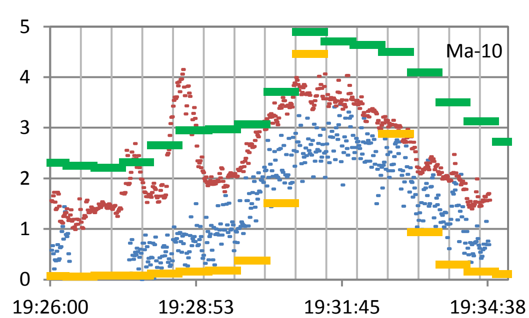
Ma-10
5
4
3
2
1
0
19:26:00
19:28:53
19:31:45
19:34:38

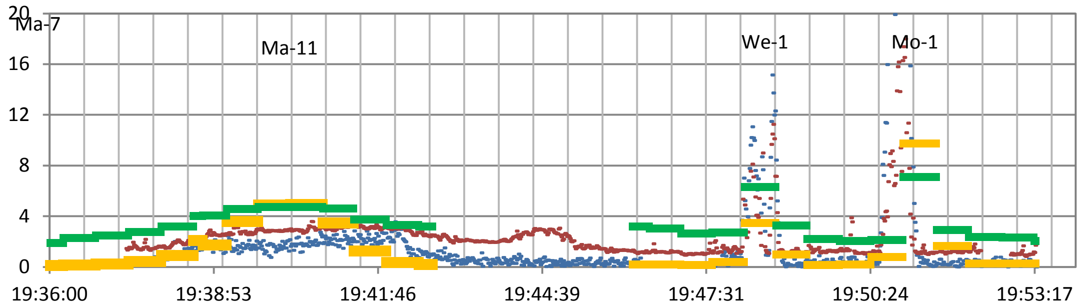
Ma-7
Ma-11
We-1
Mo-1
0
4
8
12
16
20
19:36:00
19:38:53
19:41:46
19:44:39
19:47:31
19:50:24
19:53:17

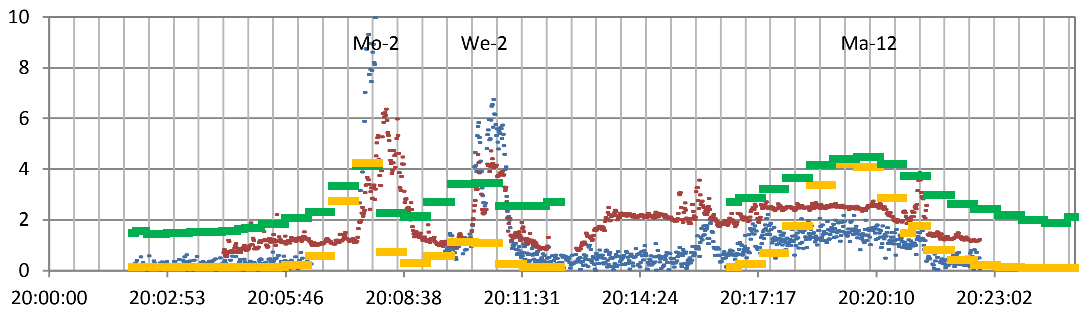
Mo-2
We-2
Ma-12
0
2
4
6
8
10
20:00:00
20:02:53
20:05:46
20:08:38
20:11:31
20:14:24
20:17:17
20:20:10
20:23:02

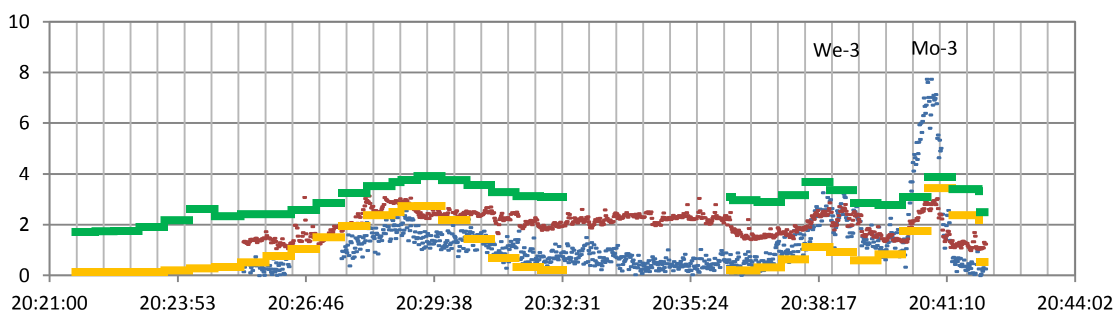
We-3
Mo-3
0
2
4
6
8
10
20:21:00
20:23:53
20:26:46
20:29:38
20:32:31
20:35:24
20:38:17
20:41:10
20:44:02

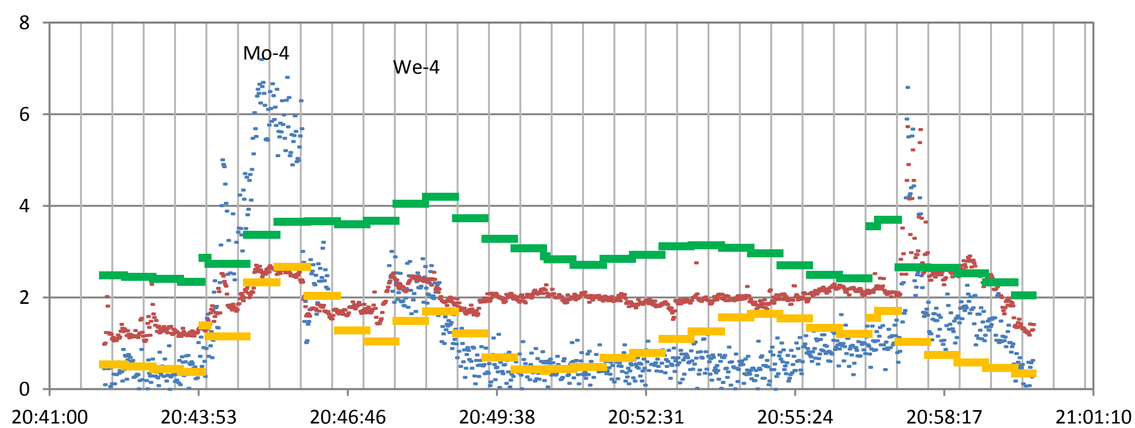
Mo-4
We-4
0
2
4
6
8
20:41:00
20:43:53
20:46:46
20:49:38
20:52:31
20:55:24
20:58:17
21:01:10

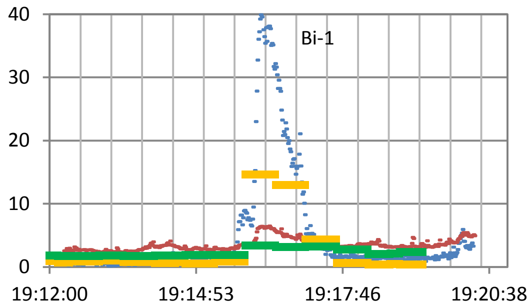
Bi-1
40
30
20
10
0
19:12:00
19:14:53
19:17:46
19:20:38

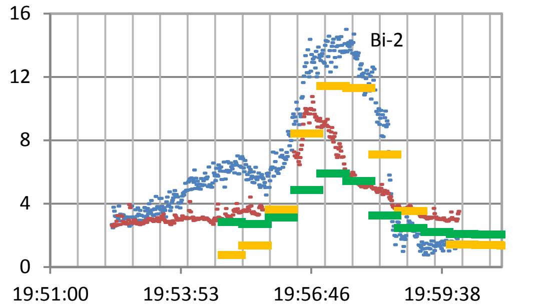
Bi-2
16
12
8
4
0
19:51:00
19:53:53
19:56:46
19:59:38

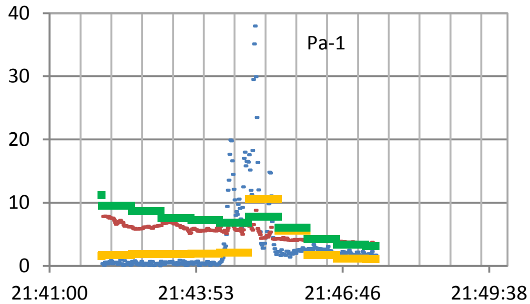
Pa-1
40
30
20
10
0
21:41:00
21:43:53
21:46:46
21:49:38

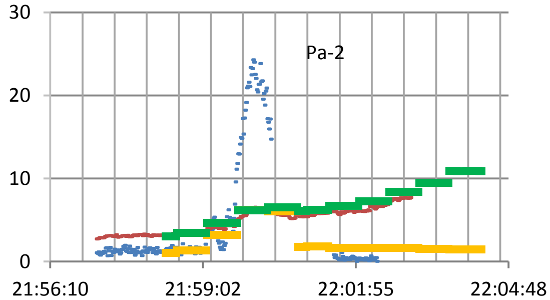
Pa-2
30
20
10
0
21:56:10
21:59:02
22:01:55
22:04:48

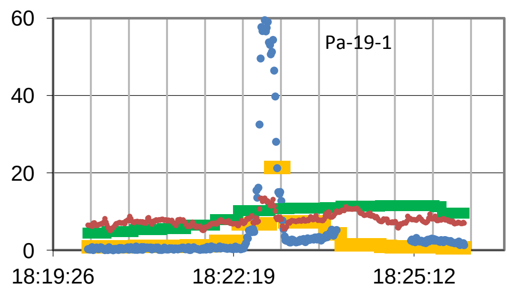
Pa-19-1
60
40
20
0
18:19:26
18:22:19
18:25:12

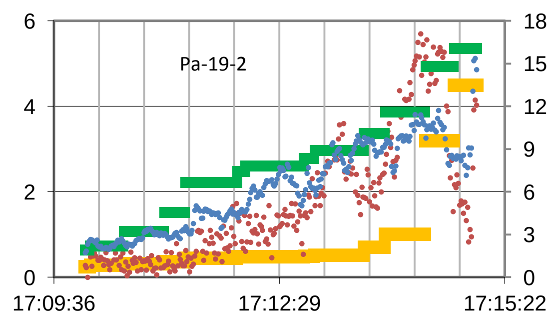
Pa-19-2
6
4
2
0
18
15
12
9
6
3
0
17:09:36
17:12:29
17:15:22

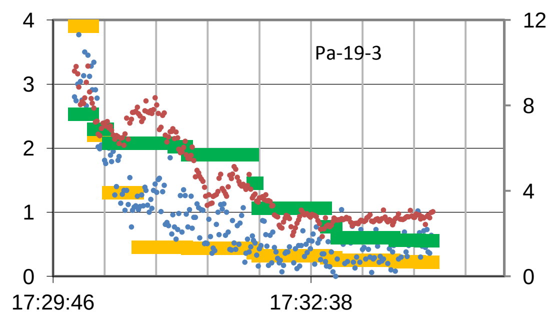
Pa-19-3
4
3
2
1
0
12
8
4
0
17:29:46
17:32:38

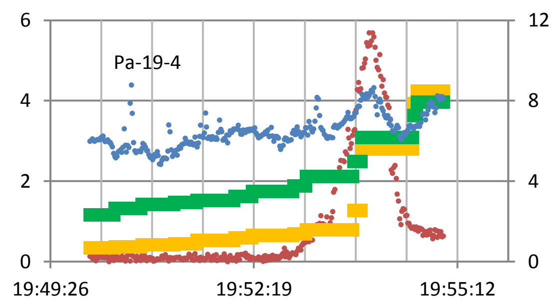
Pa-19-4
6
4
2
0
12
8
4
0
19:49:26
19:52:19
19:55:12

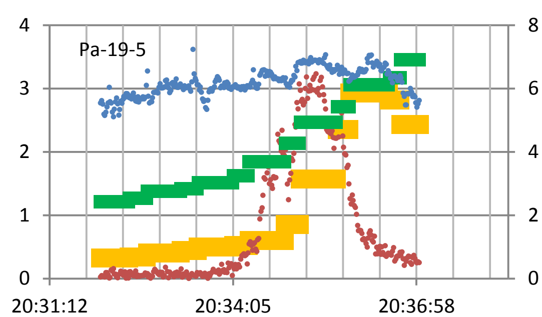
Pa-19-5
4
3
2
1
0
8
6
4
2
0
20:31:12
20:34:05
20:36:58

Fig. S1. Comparison of modeled SO_2 (yellow flat line) and NO_y (green flat line) to the observed SO_2 (blue dot) and NO_y (red dots) at each plume transect on September 16, 19 and 25. Horizontal coordinate is time scale in GMT (local time = GMT - 6 hours) and vertical coordinate is concentration (ppb). Transect names listed in Table S3 of the manuscript are labled in each subplot.

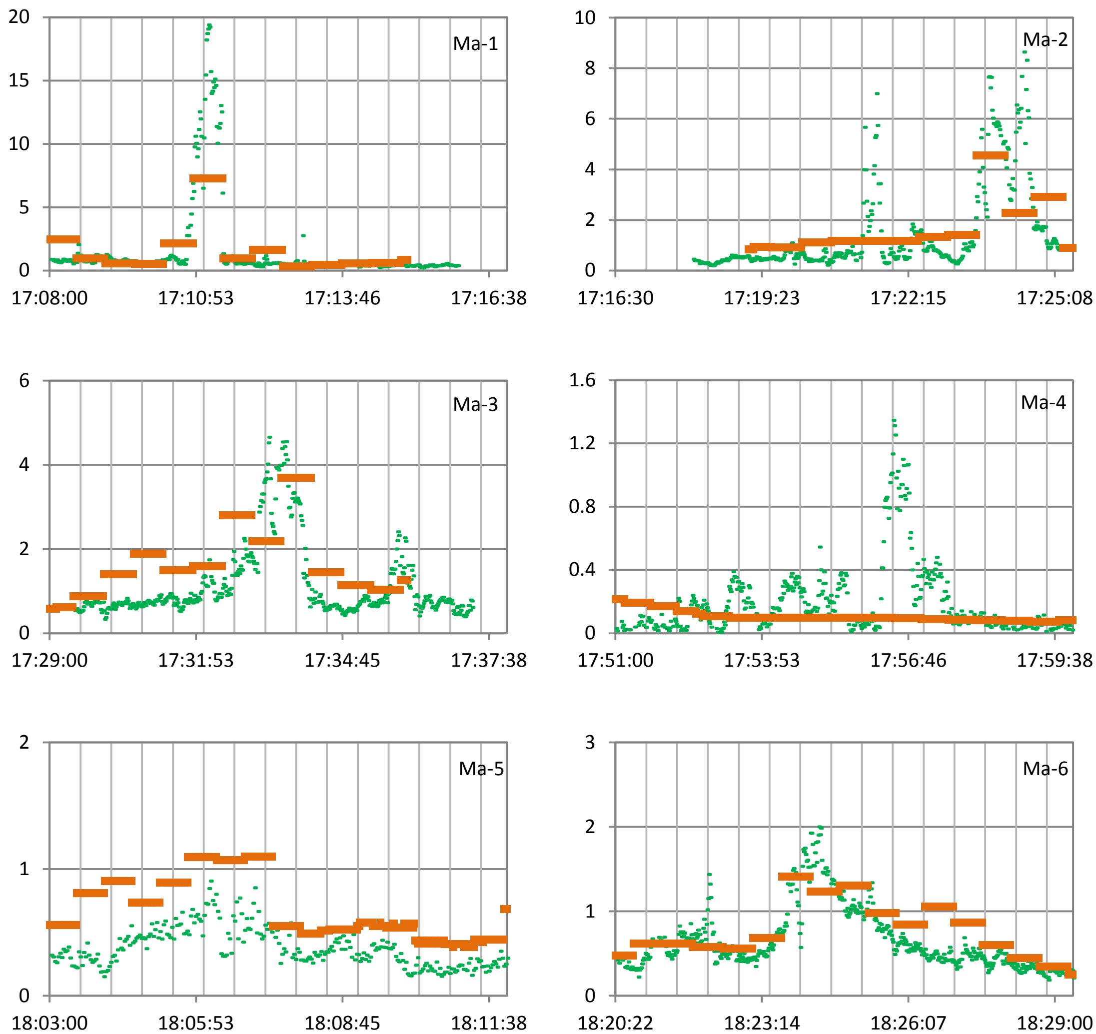

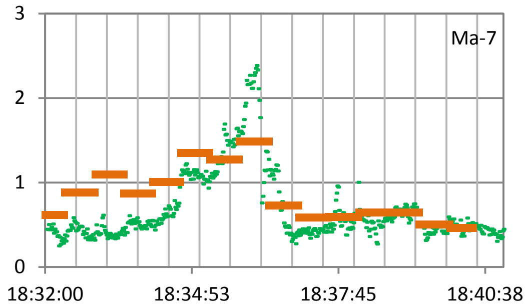
Ma-7
3
2
1
0
18:32:00
18:34:53
18:37:45
18:40:38

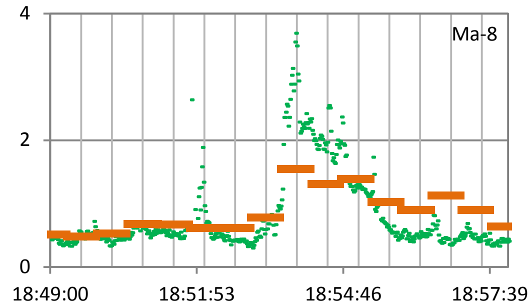
Ma-8
4
2
0
18:49:00
18:51:53
18:54:46
18:57:39

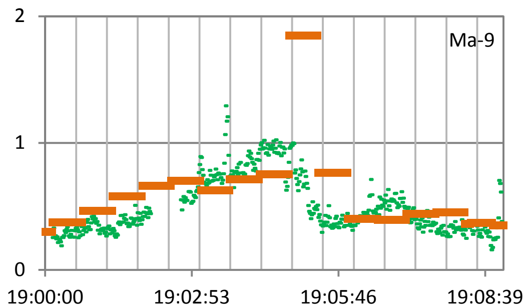
Ma-9
2
1
0
19:00:00
19:02:53
19:05:46
19:08:39

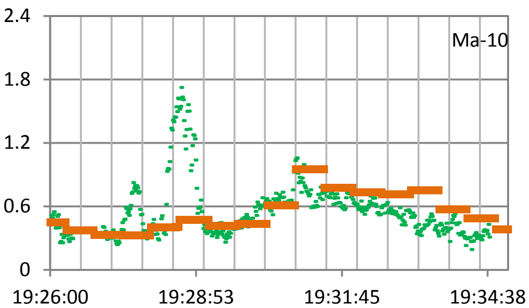
Ma-10
2.4
1.8
1.2
0.6
0
19:26:00
19:28:53
19:31:45
19:34:38

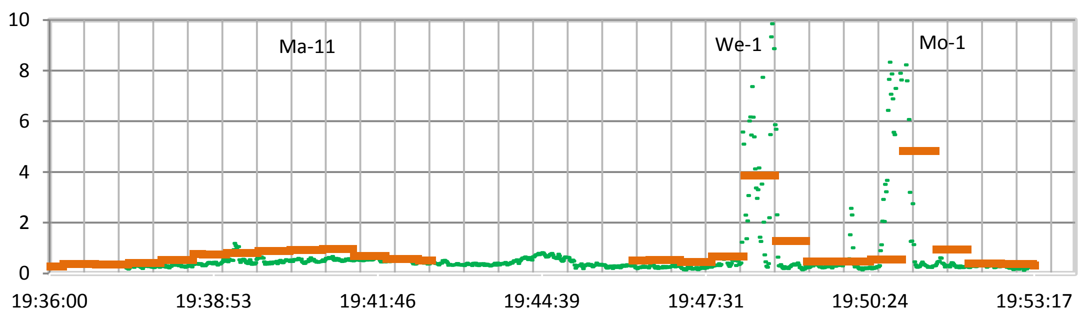
Ma-11
We-1
Mo-1
10
8
6
4
2
0
19:36:00
19:38:53
19:41:46
19:44:39
19:47:31
19:50:24
19:53:17

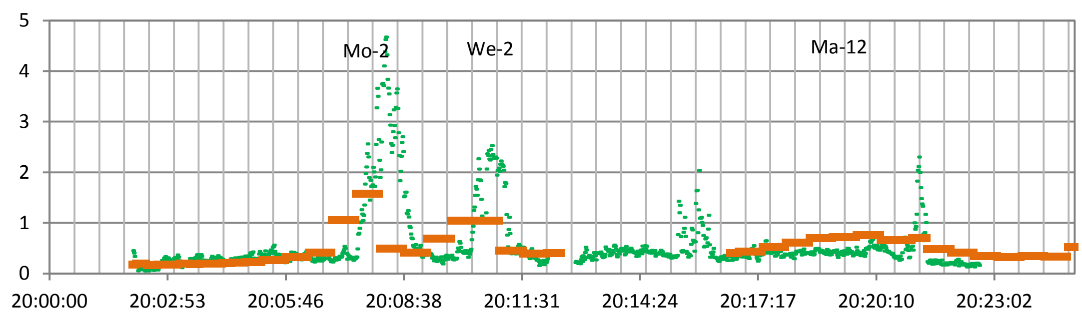
Mo-2
We-2
Ma-12
5
4
3
2
1
0
20:00:00
20:02:53
20:05:46
20:08:38
20:11:31
20:14:24
20:17:17
20:20:10
20:23:02

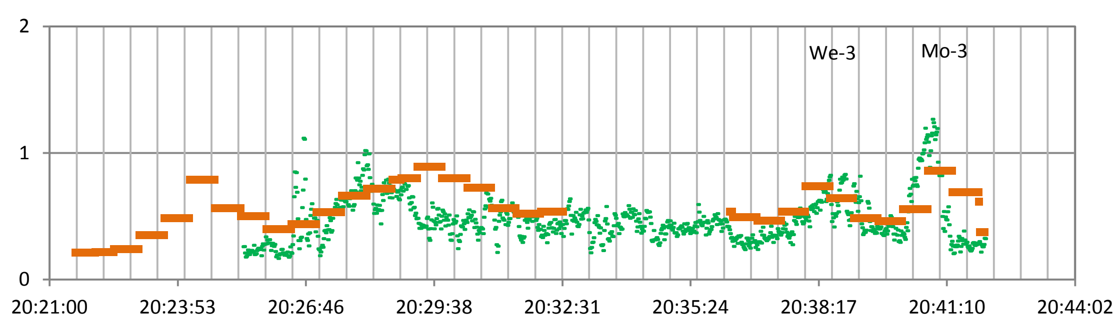
We-3
Mo-3
2
1
0
20:21:00
20:23:53
20:26:46
20:29:38
20:32:31
20:35:24
20:38:17
20:41:10
20:44:02

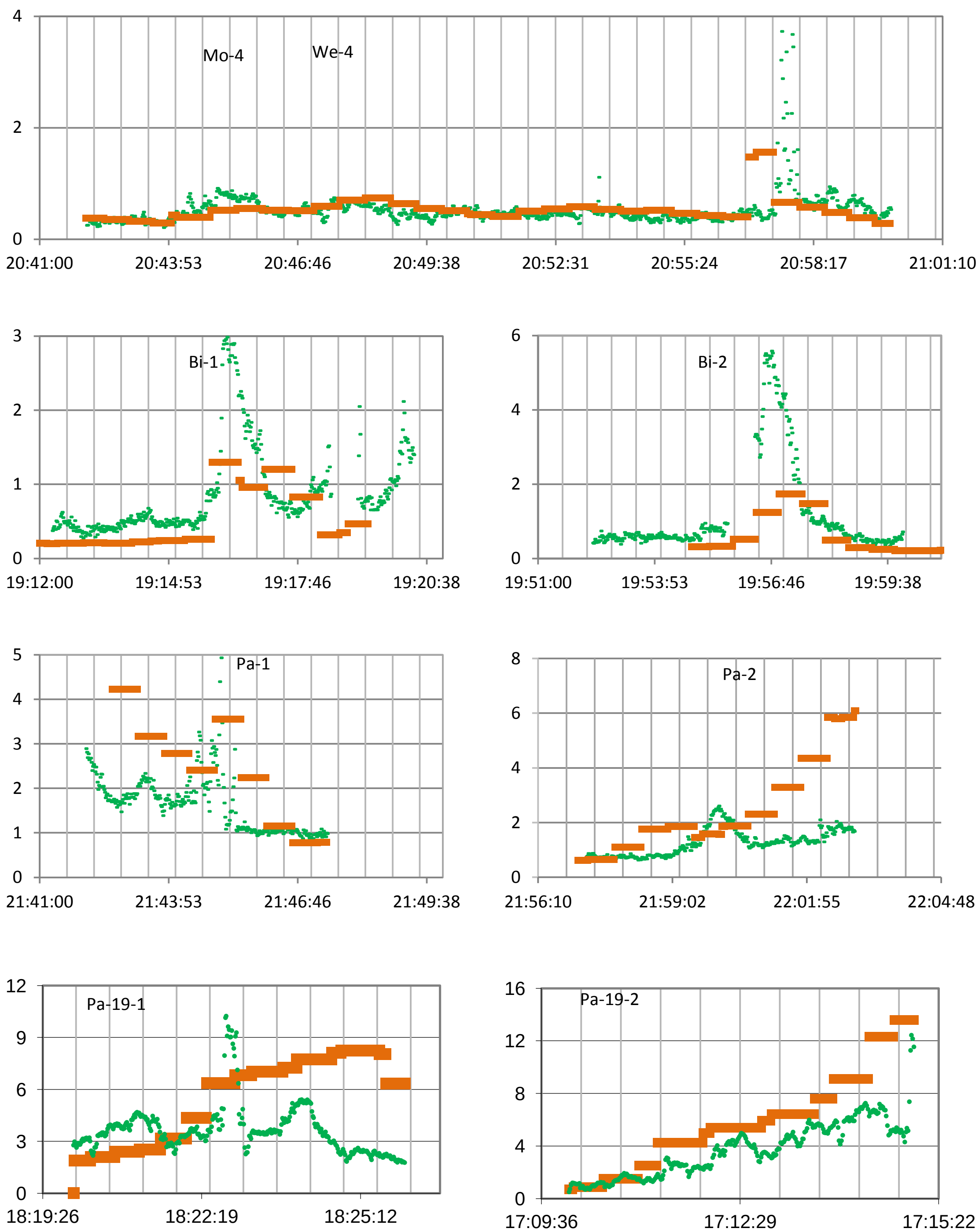
Mo-4
We-4
0
2
4
20:41:00
20:43:53
20:46:46
20:49:38
20:52:31
20:55:24
20:58:17
21:01:10
Bi-1
0
1
2
3
19:12:00
19:14:53
19:17:46
19:20:38
Bi-2
0
2
4
6
19:51:00
19:53:53
19:56:46
19:59:38
Pa-1
0
1
2
3
4
5
21:41:00
21:43:53
21:46:46
21:49:38
Pa-2
0
2
4
6
8
21:56:10
21:59:02
22:01:55
22:04:48
Pa-19-1
0
3
6
9
12
18:19:26
18:22:19
18:25:12
Pa-19-2
0
4
8
12
16
17:09:36
17:12:29
17:15:22

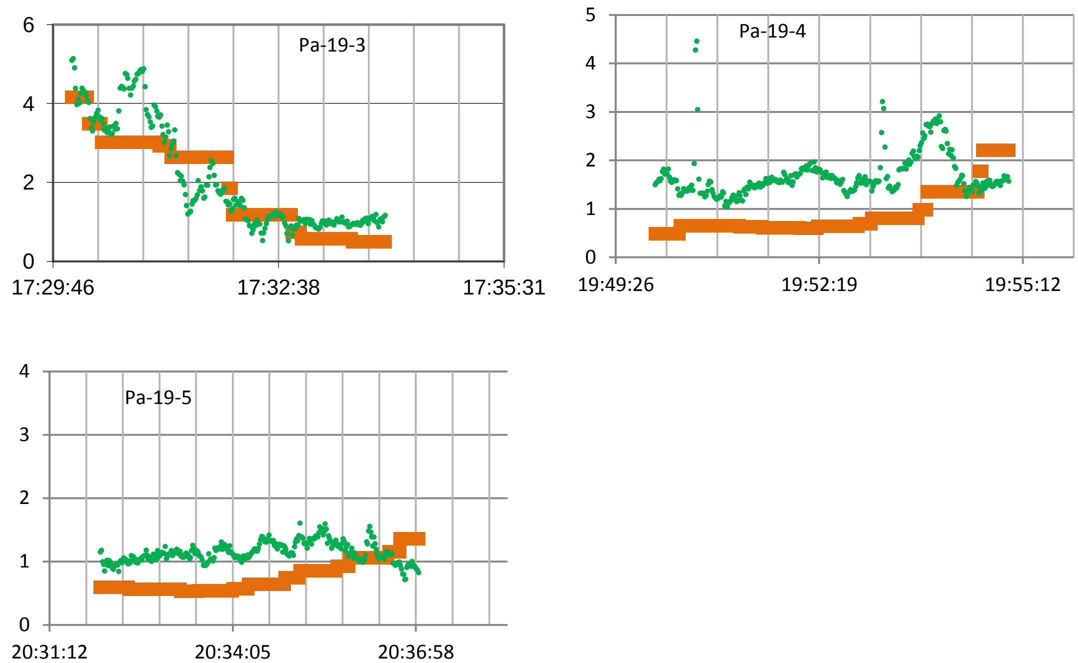

Fig. S2. Comparison of the modeled NO_x (orange flat line) to the observed NO_x (green dot) at each plume transect on September 16, 19 and 25. Horizontal coordinate is time in GMT (local time = GMT - 6 hours) and vertical coordinate is concentration (ppb). Transect names listed in Table S3 of the manuscript are labled in each subplot.

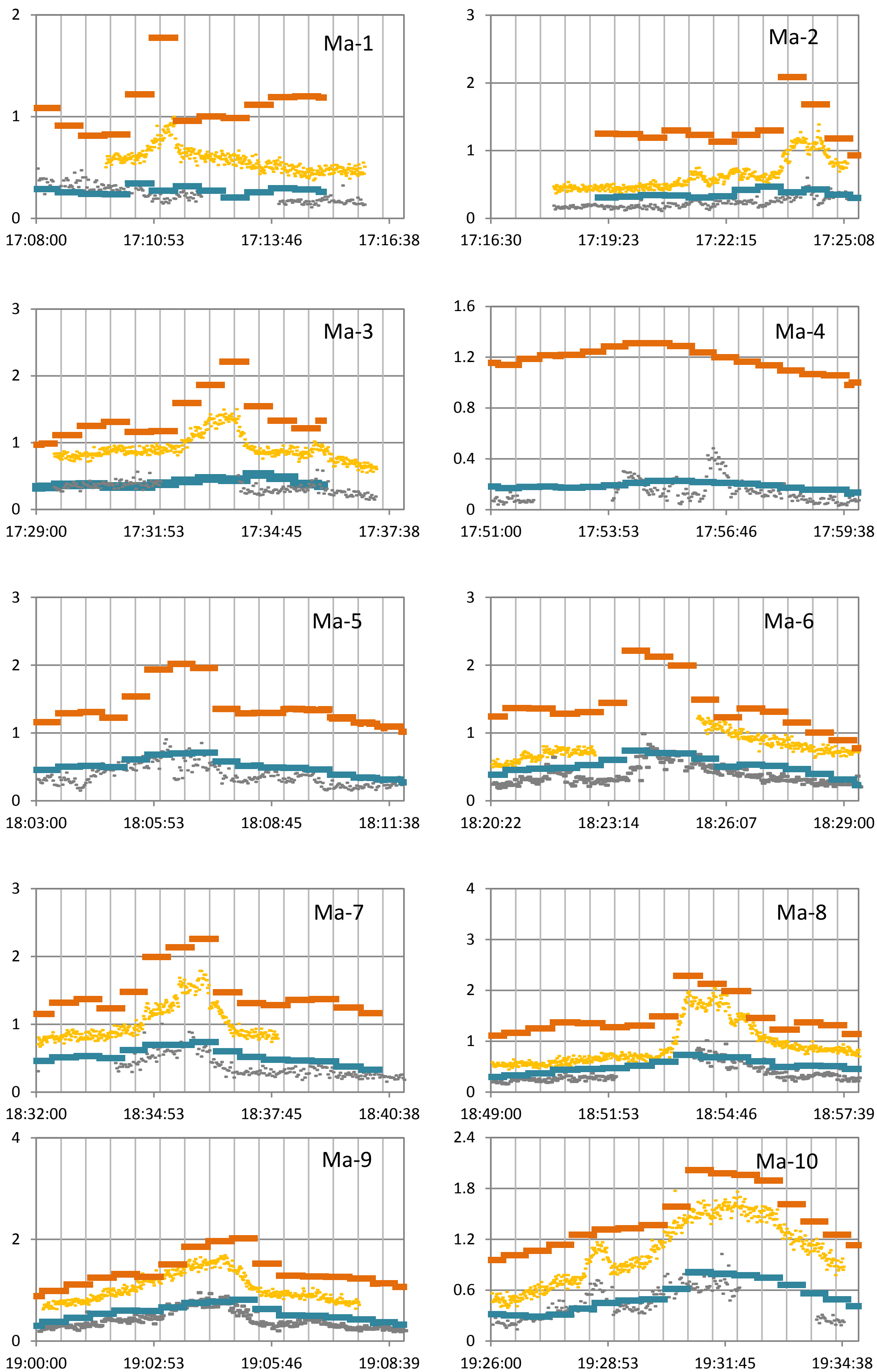
Ma-1
2
1
0
17:08:00
17:10:53
17:13:46
17:16:38
Ma-2
3
2
1
0
17:16:30
17:19:23
17:22:15
17:25:08
Ma-3
3
2
1
0
17:29:00
17:31:53
17:34:45
17:37:38
Ma-4
1.6
1.2
0.8
0.4
0
17:51:00
17:53:53
17:56:46
17:59:38
Ma-5
3
2
1
0
18:03:00
18:05:53
18:08:45
18:11:38
Ma-6
3
2
1
0
18:20:22
18:23:14
18:26:07
18:29:00
Ma-7
3
2
1
0
18:32:00
18:34:53
18:37:45
18:40:38
Ma-8
4
3
2
1
0
18:49:00
18:51:53
18:54:46
18:57:39
Ma-9
4
2
0
19:00:00
19:02:53
19:05:46
19:08:39
Ma-10
2.4
1.8
1.2
0.6
0
19:26:00
19:28:53
19:31:45
19:34:38

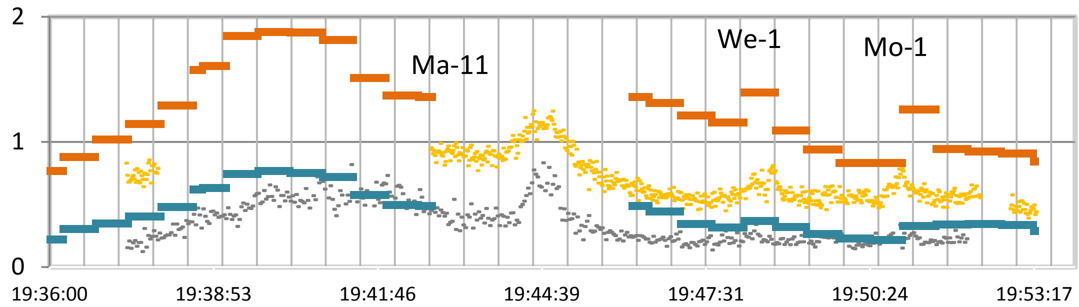
2
1
0
19:36:00
19:38:53
19:41:46
19:44:39
19:47:31
19:50:24
19:53:17
Ma-11
We-1
Mo-1

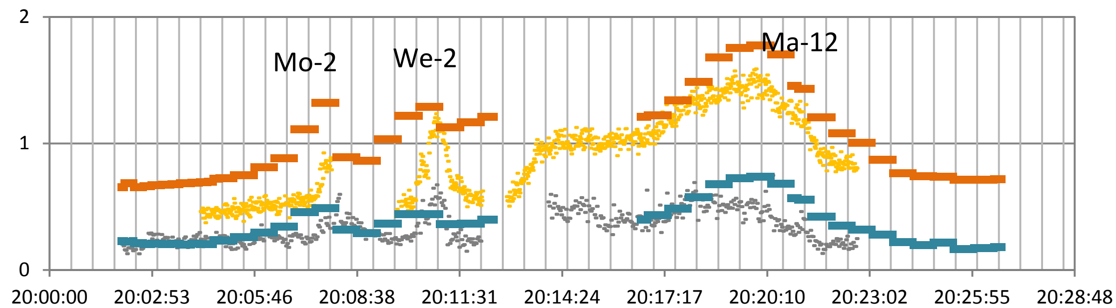
2
1
0
20:00:00
20:02:53
20:05:46
20:08:38
20:11:31
20:14:24
20:17:17
20:20:10
20:23:02
20:25:55
20:28:48
Mo-2
We-2
Ma-12

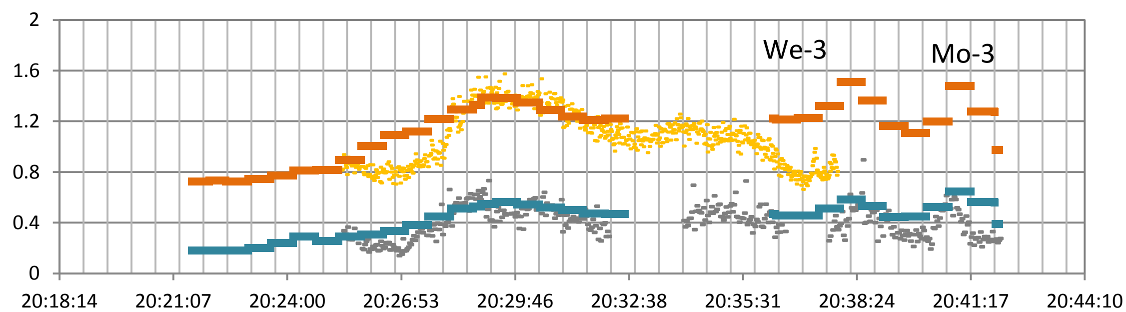
2
1.6
1.2
0.8
0.4
0
20:18:14
20:21:07
20:24:00
20:26:53
20:29:46
20:32:38
20:35:31
20:38:24
20:41:17
20:44:10
We-3
Mo-3

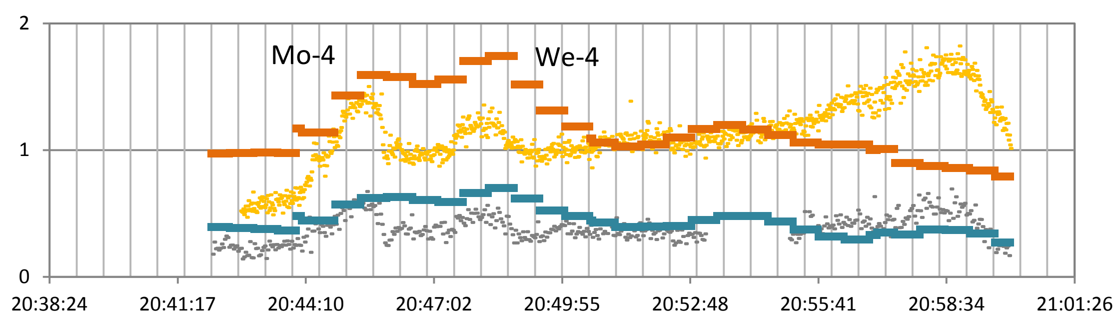
2
1
0
20:38:24
20:41:17
20:44:10
20:47:02
20:49:55
20:52:48
20:55:41
20:58:34
21:01:26
Mo-4
We-4

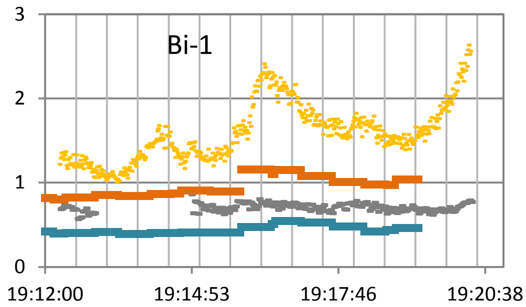
Bi-1
0
1
2
3
19:12:00
19:14:53
19:17:46
19:20:38

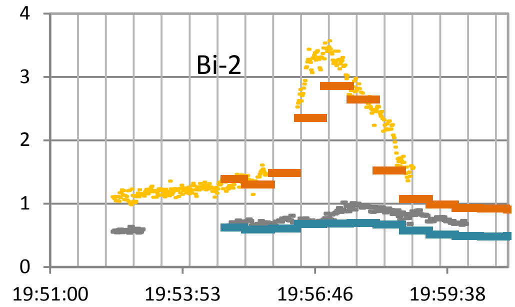
Bi-2
0
1
2
3
4
19:51:00
19:53:53
19:56:46
19:59:38

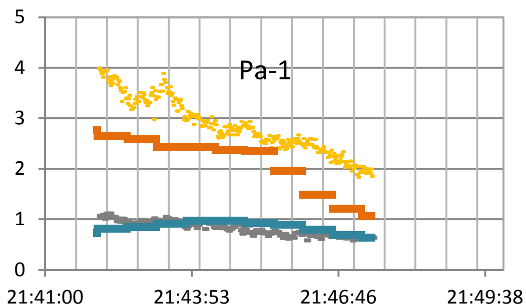
Pa-1
0
1
2
3
4
5
21:41:00
21:43:53
21:46:46
21:49:38

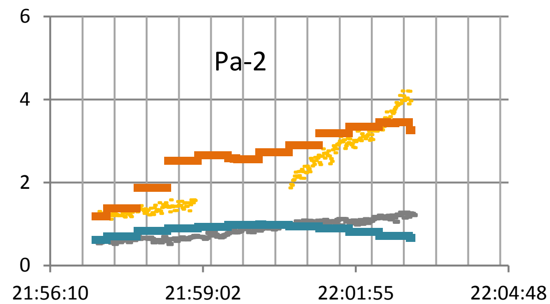
Pa-2
0
2
4
6
21:56:10
21:59:02
22:01:55
22:04:48

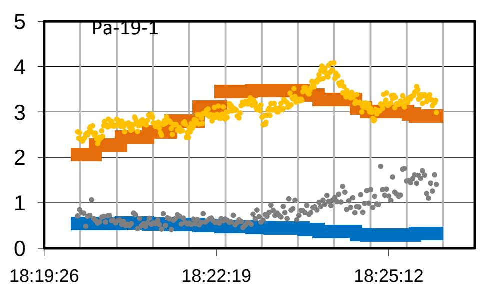
Pa-19-1
0
1
2
3
4
5
18:19:26
18:22:19
18:25:12

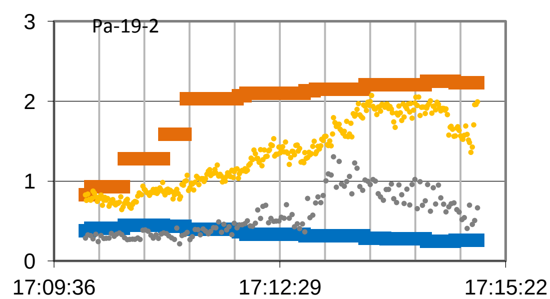
Pa-19-2
0
1
2
3
17:09:36
17:12:29
17:15:22

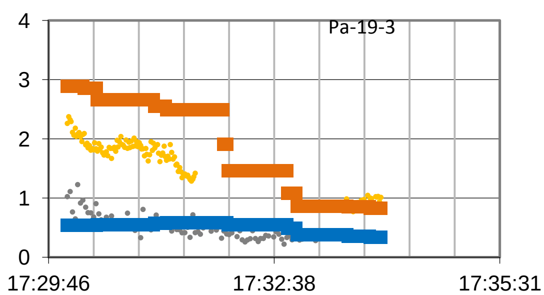
Pa-19-3
0
1
2
3
4
17:29:46
17:32:38
17:35:31

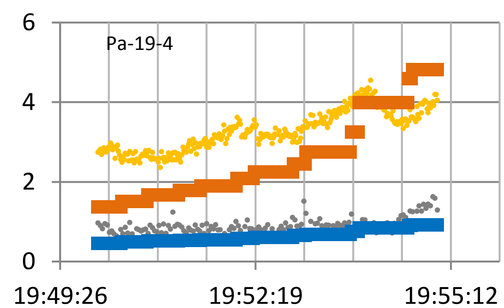
Pa-19-4
0
2
4
6
19:49:26
19:52:19
19:55:12

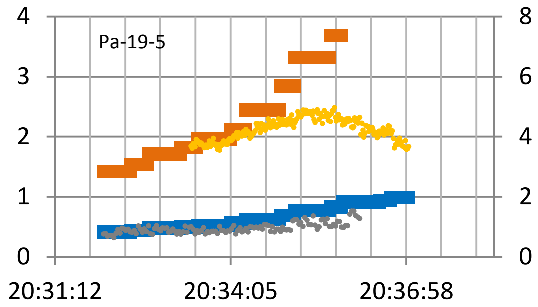

Fig. S3. Comparison of the modeled HNO_3 (orange flat line) and PAN (aqua flat line) to the observed HNO_3 (yellow dot) and PAN (gray dot) at each plume transect on September 16, 19 and 25. Horizontal coordinate is time in GMT (local time = GMT - 6 hours) and vertical coordinate is concentration (ppb). Transect names listed in Table S3 of the manuscript are labeled in each subplot.

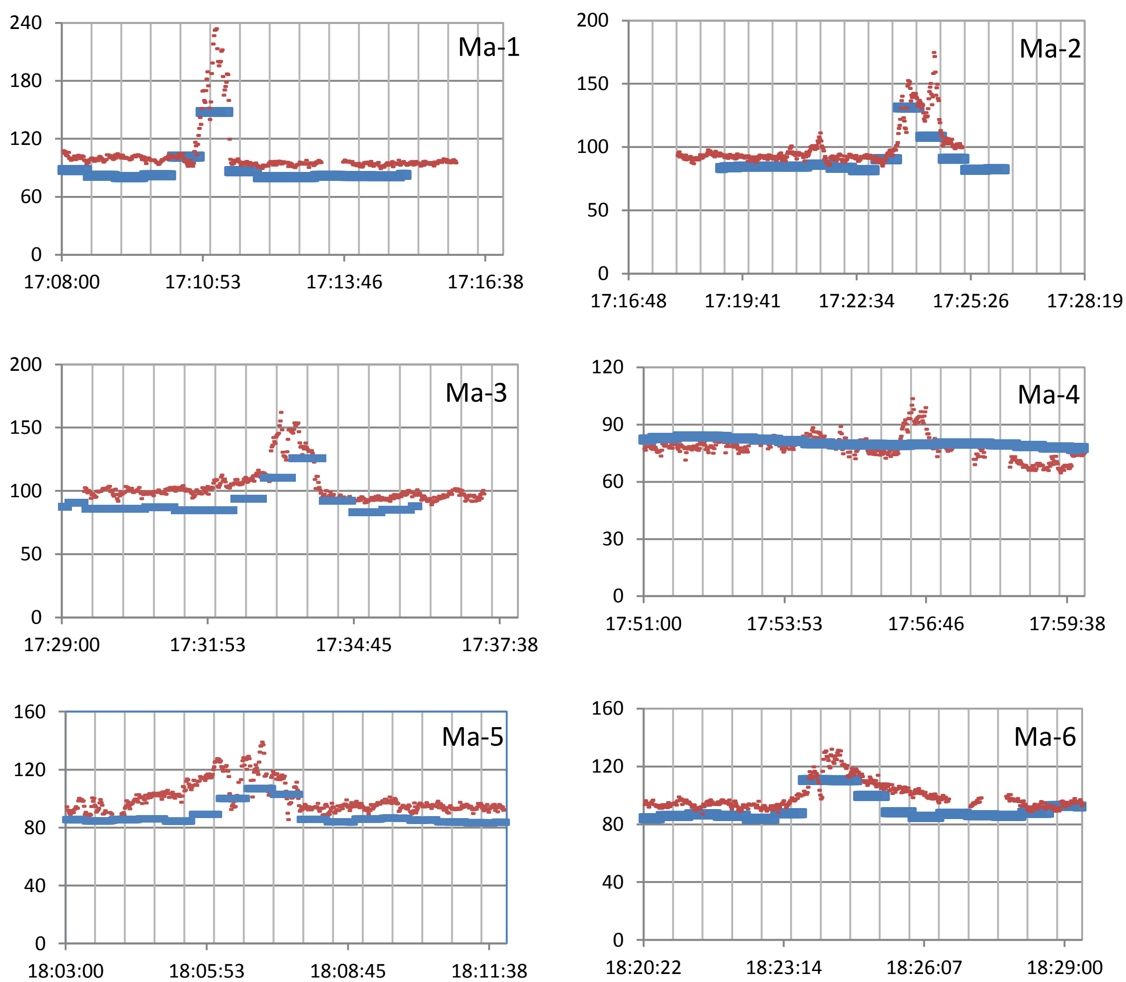

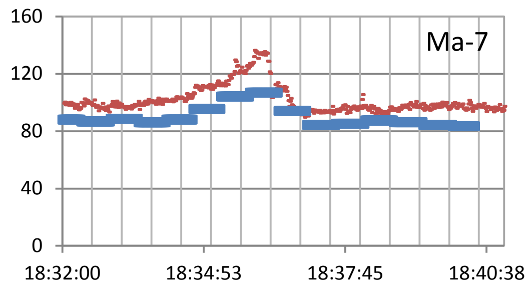
Ma-7
160
120
80
40
0
18:32:00
18:34:53
18:37:45
18:40:38

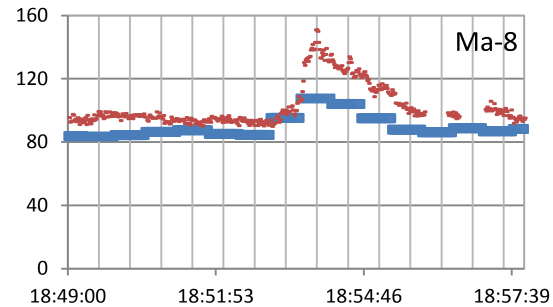
Ma-8
160
120
80
40
0
18:49:00
18:51:53
18:54:46
18:57:39

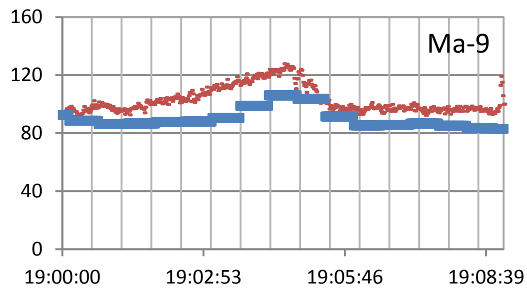
Ma-9
160
120
80
40
0
19:00:00
19:02:53
19:05:46
19:08:39

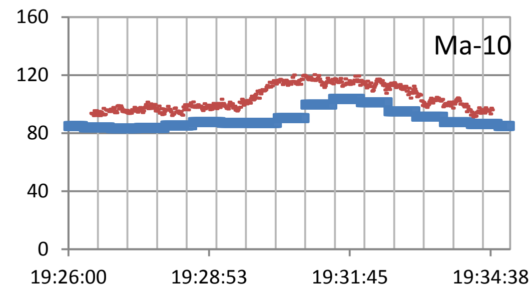
Ma-10
160
120
80
40
0
19:26:00
19:28:53
19:31:45
19:34:38

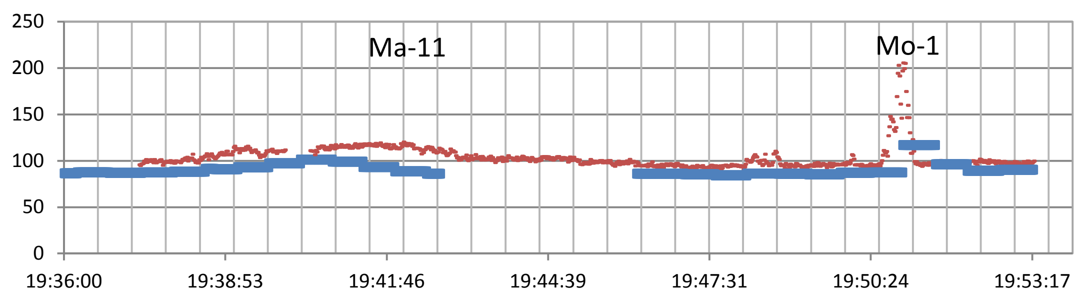
Ma-11
Mo-1
250
200
150
100
50
0
19:36:00
19:38:53
19:41:46
19:44:39
19:47:31
19:50:24
19:53:17

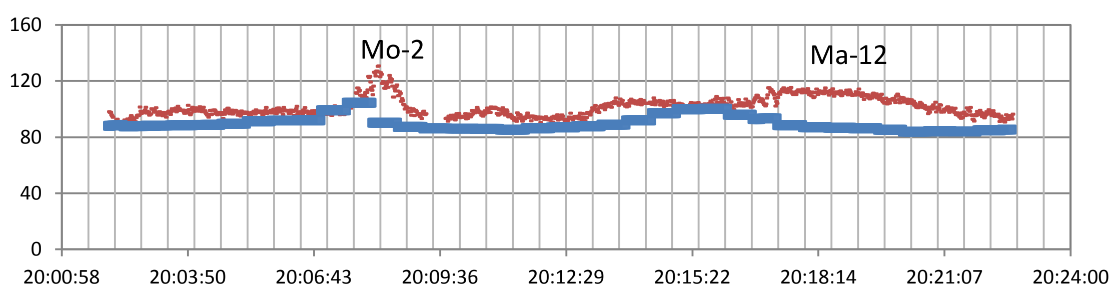
Mo-2
Ma-12
160
120
80
40
0
20:00:58
20:03:50
20:06:43
20:09:36
20:12:29
20:15:22
20:18:14
20:21:07
20:24:00

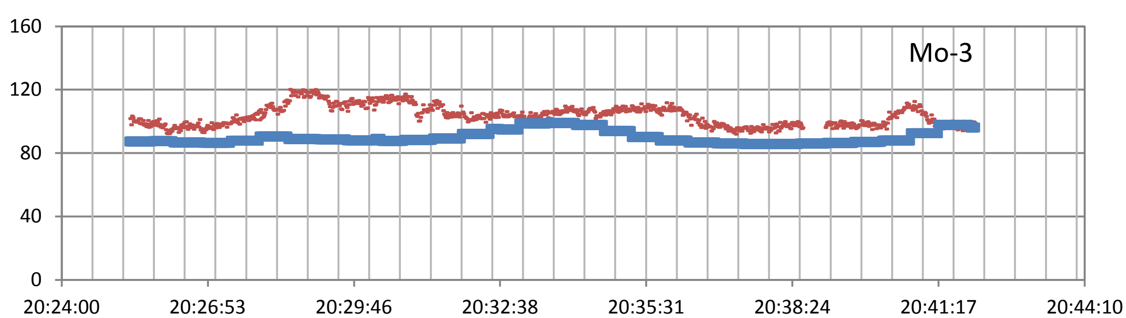
Mo-3
160
120
80
40
0
20:24:00
20:26:53
20:29:46
20:32:38
20:35:31
20:38:24
20:41:17
20:44:10

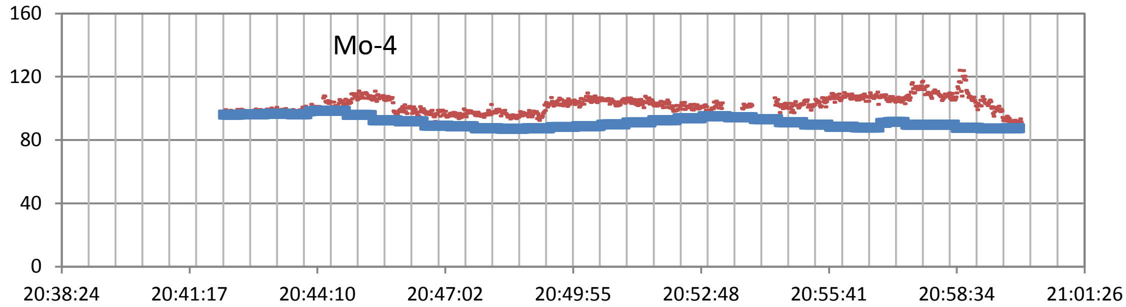
Mo-4
160
120
80
40
0
20:38:24
20:41:17
20:44:10
20:47:02
20:49:55
20:52:48
20:55:41
20:58:34
21:01:26

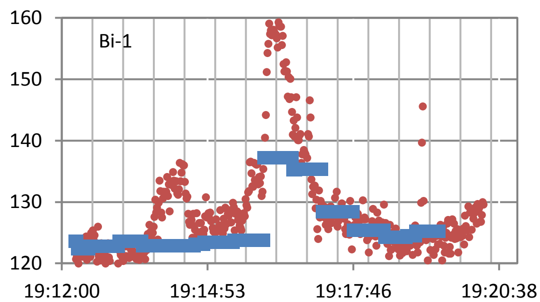
Bi-1
160
150
140
130
120
19:12:00
19:14:53
19:17:46
19:20:38

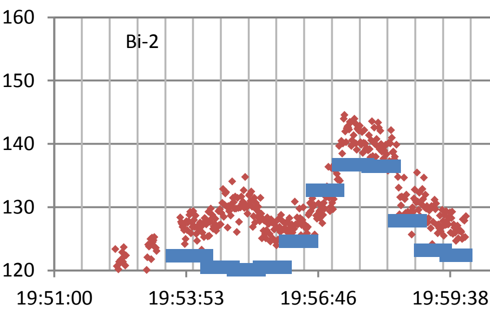
Bi-2
160
150
140
130
120
19:51:00
19:53:53
19:56:46
19:59:38

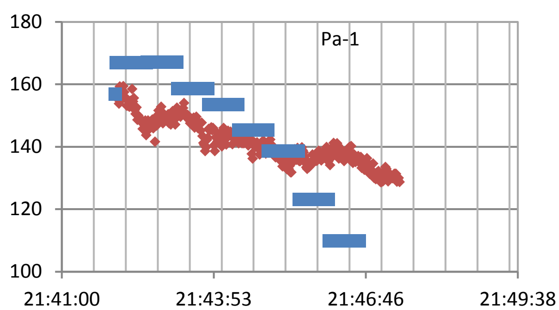
Pa-1
180
160
140
120
100
21:41:00
21:43:53
21:46:46
21:49:38

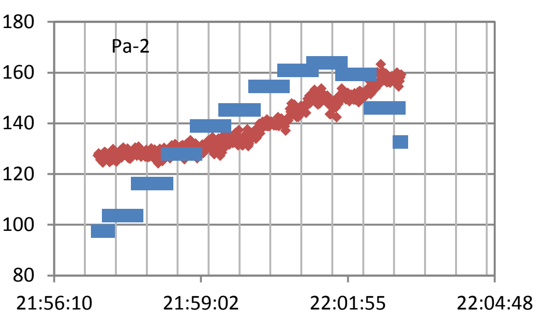
Pa-2
180
160
140
120
100
80
21:56:10
21:59:02
22:01:55
22:04:48

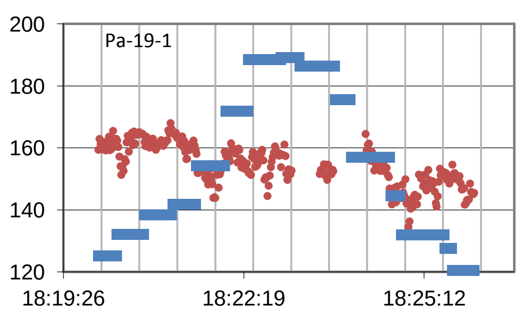
Pa-19-1
200
180
160
140
120
18:19:26
18:22:19
18:25:12

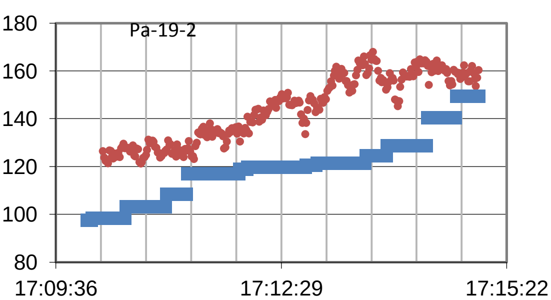
Pa-19-2
180
160
140
120
100
80
17:09:36
17:12:29
17:15:22

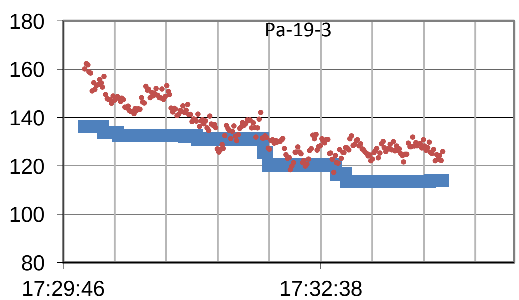
Pa-19-3
180
160
140
120
100
80
17:29:46
17:32:38

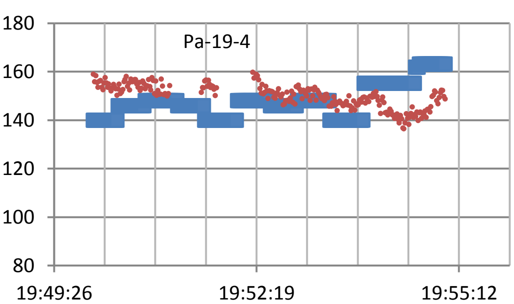
Pa-19-4
180
160
140
120
100
80
19:49:26
19:52:19
19:55:12

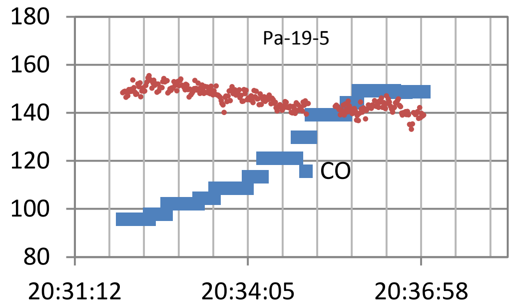

Fig. S4. Comparison of the modeled CO (blue flat line) to the observed CO (red dot) at each plume transect on September 16, 19 and 25. Horizontal coordinate is time in GMT (local time = GMT - 6 hours) and vertical coordinate is concentration (ppb). Transect names listed in Table S3 of the manuscript are labled in each subplot.

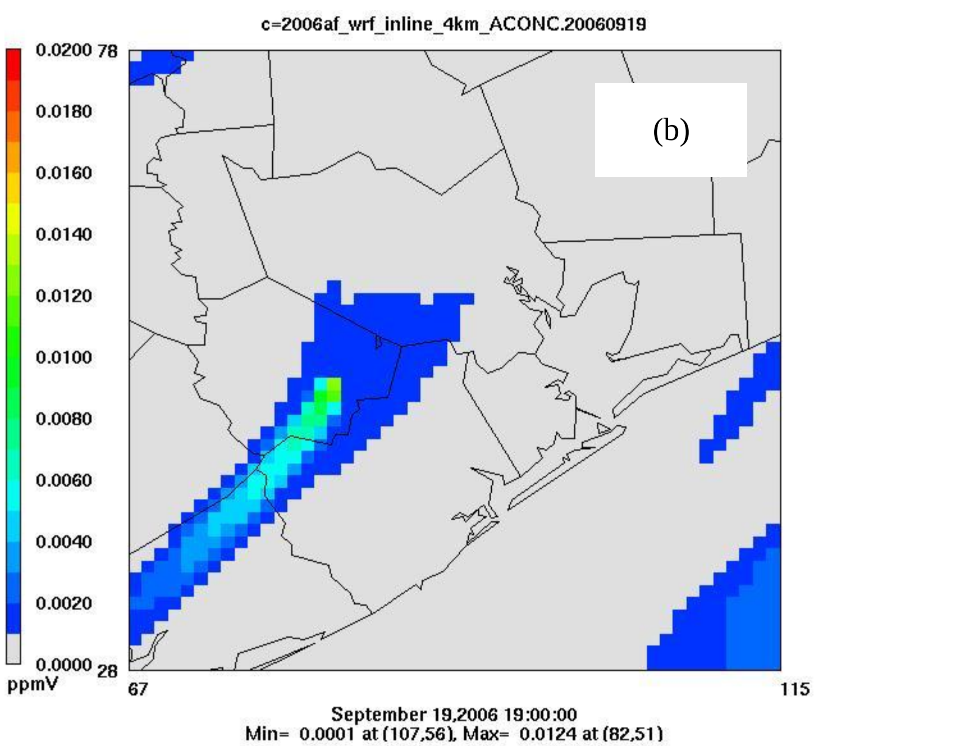

Fig. S5. (a) Observed PPPs of Parish on September 19, 2006. The red star show the locations of the Parish plant. (b) Simulated PPPs of Parish at 19:00 GMT (local time: 13:00)

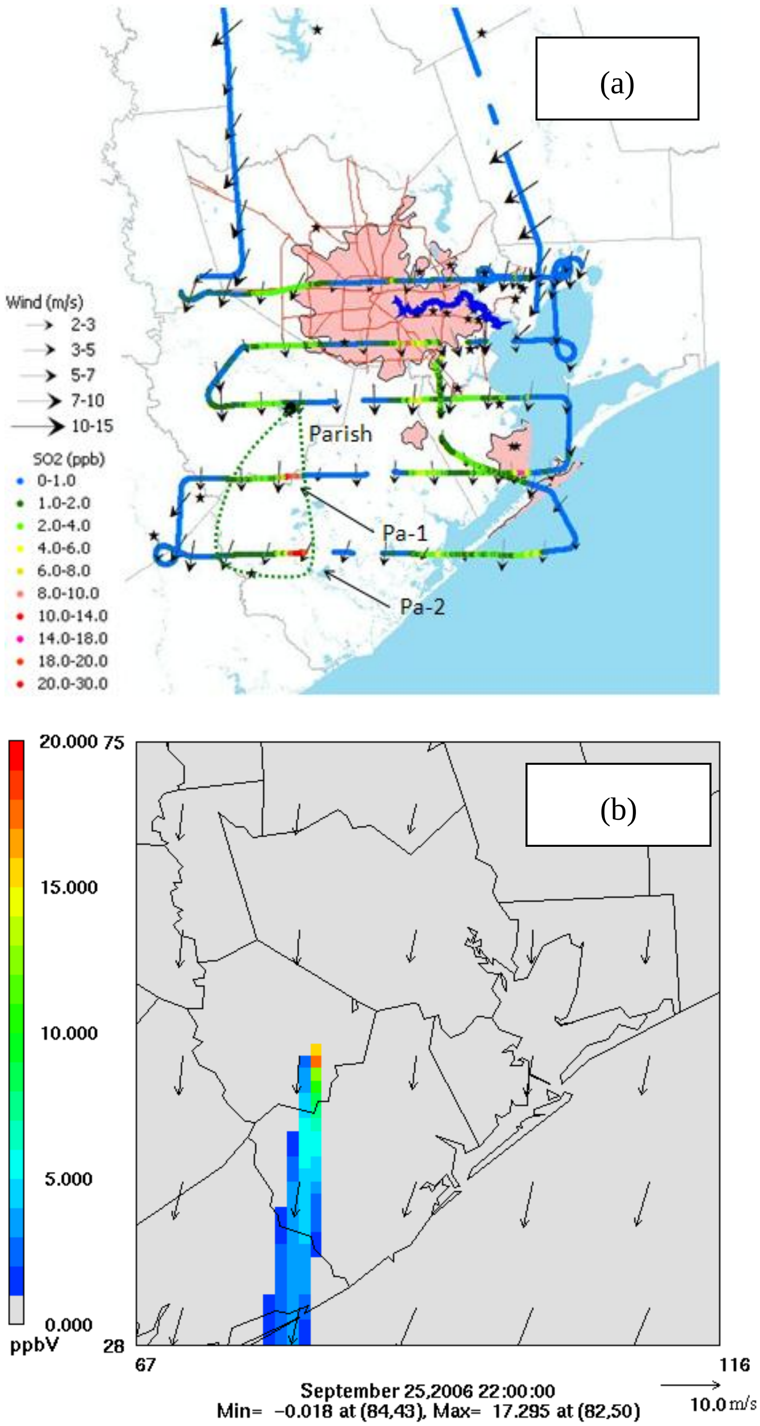

(a)
Wind (m/s)
2-3
3-5
5-7
7-10
10-15
SO2 (ppb)
0-1.0
1.0-2.0
2.0-4.0
4.0-6.0
6.0-8.0
8.0-10.0
10.0-14.0
14.0-18.0
18.0-20.0
20.0-30.0
Parish
Pa-1
Pa-2
(b)
20.000
15.000
10.000
5.000
0.000
ppbV
75
28
67
116
September 25,2006 22:00:00
Min= -0.018 at (84,43), Max= 17.295 at (82,50)
10.0 m/s

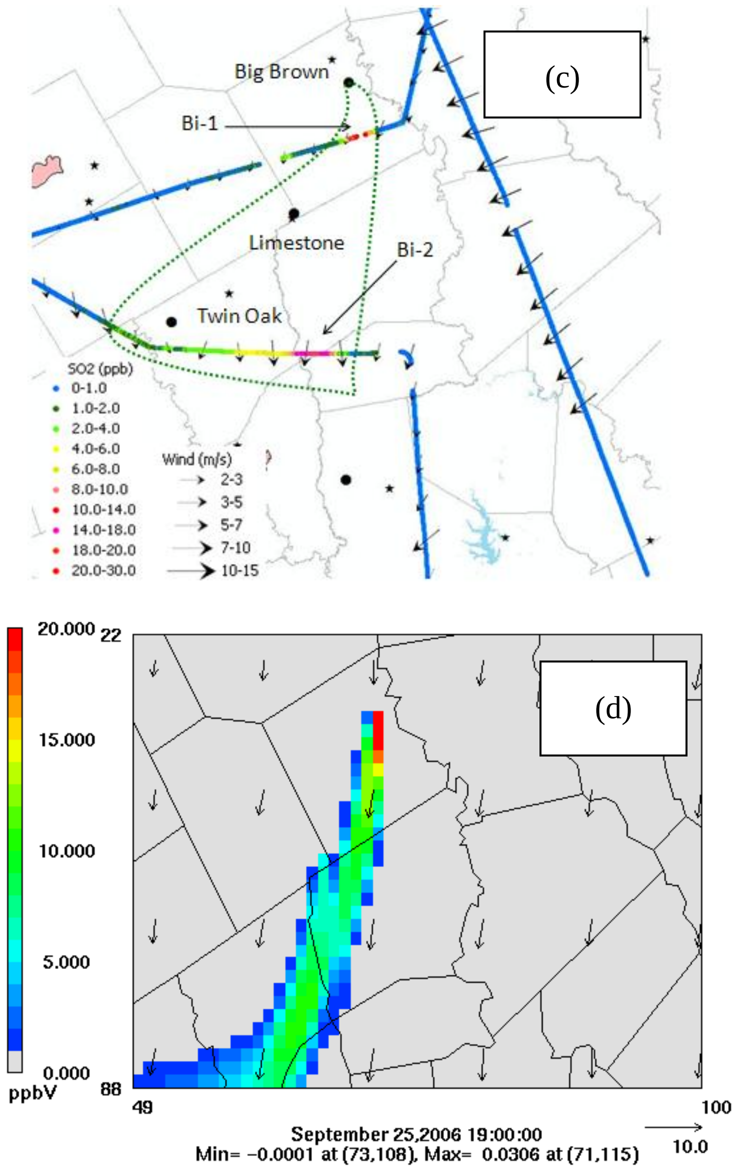

Fig. S6. (a) Observed PPPs of Parish on September 25, 2006. The black dots show the locations of the power plants. PPPs are identified by measured SO_2 enhancement (color gradient in the figure), are outlined using green dash lines. Measured wind vectors are presented on the plume transect. (b) Simulated PPPs of Parish at 22:00 GMT (local time: 16:00). (c) Observed PPPs of Big Brown and Limestone on September 25, 2006. The black dots show the locations of the power plants. PPPs are identified by measured SO_2 enhancement (color gradient in the figure), are outlined using green dash lines. Measured winds vectors are presented on the plume transect. (d) Simulated PPPs of Big Brown and Limestone at 19:00 GMT (local time: 13:00)

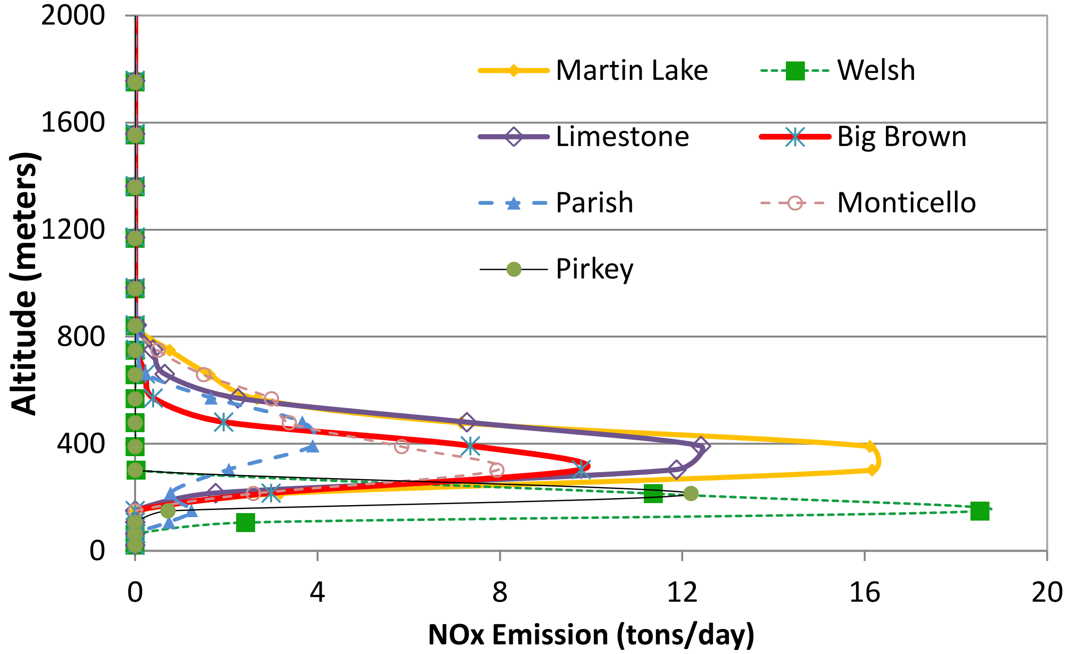

Fig. S7. Vertical distribution of NO_x for power plants simulated by CMAQ inline v4.7 on the day of measurement.

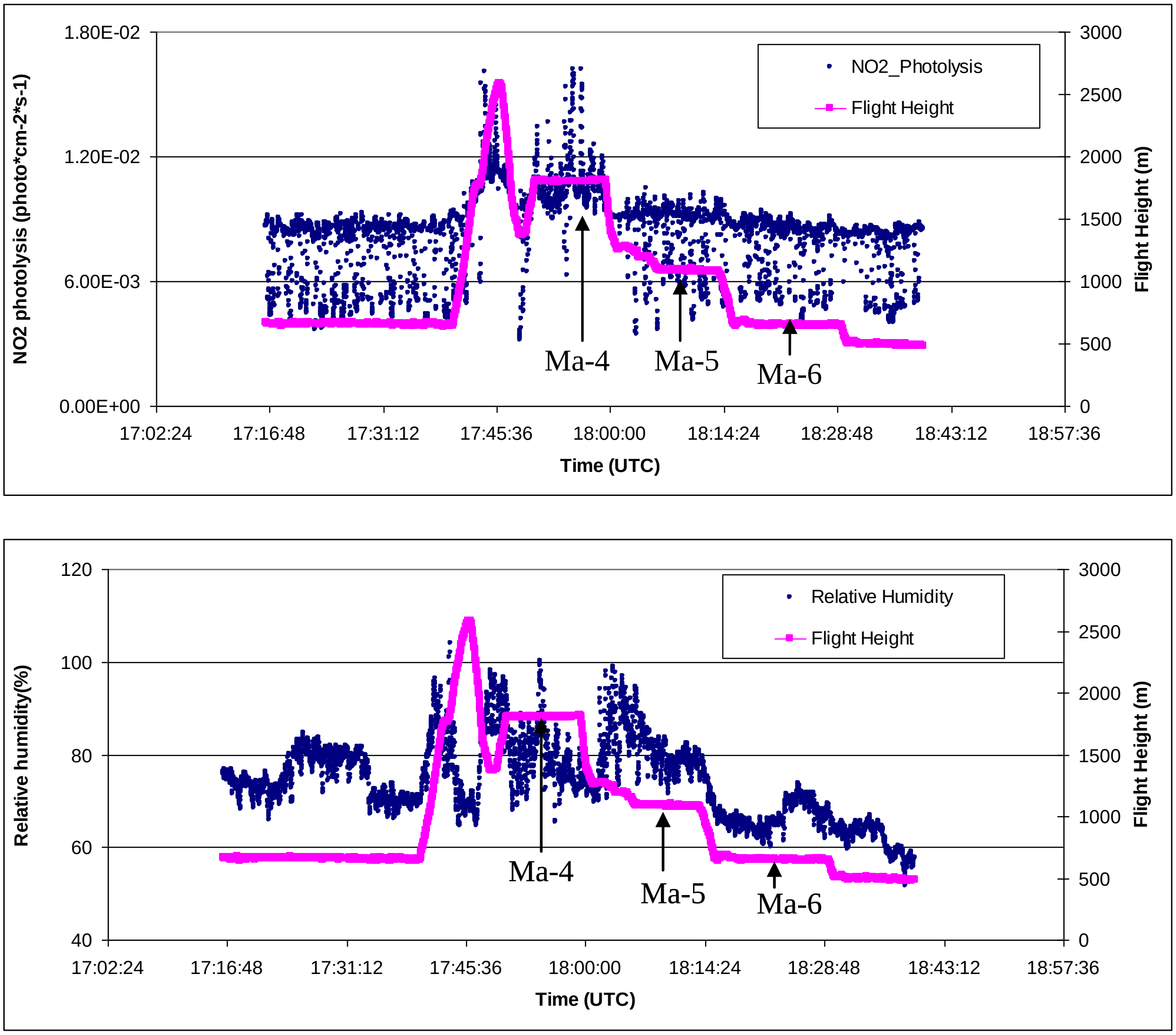

Fig. S8 (a) the observed photolysis rate (left axis, blue dot) and the flight height (right axis, black line). (b) the observed relative humidity (right axis, black cross) and the flight height (left axis, blue line). The corresponding plume transects (Table 3 and Fig. 2) are marked.

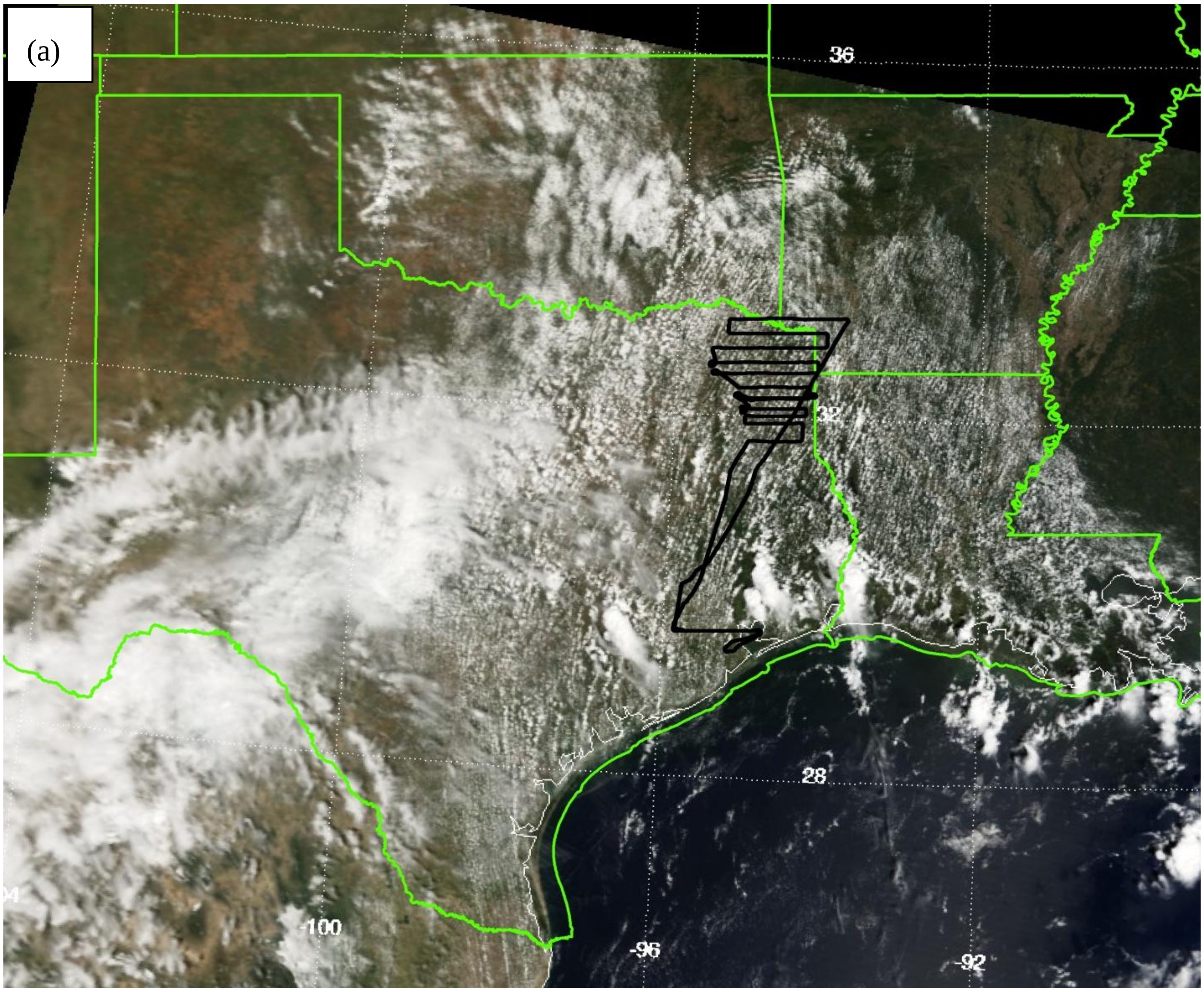

(a)
36
32
28
-100
-96
-92

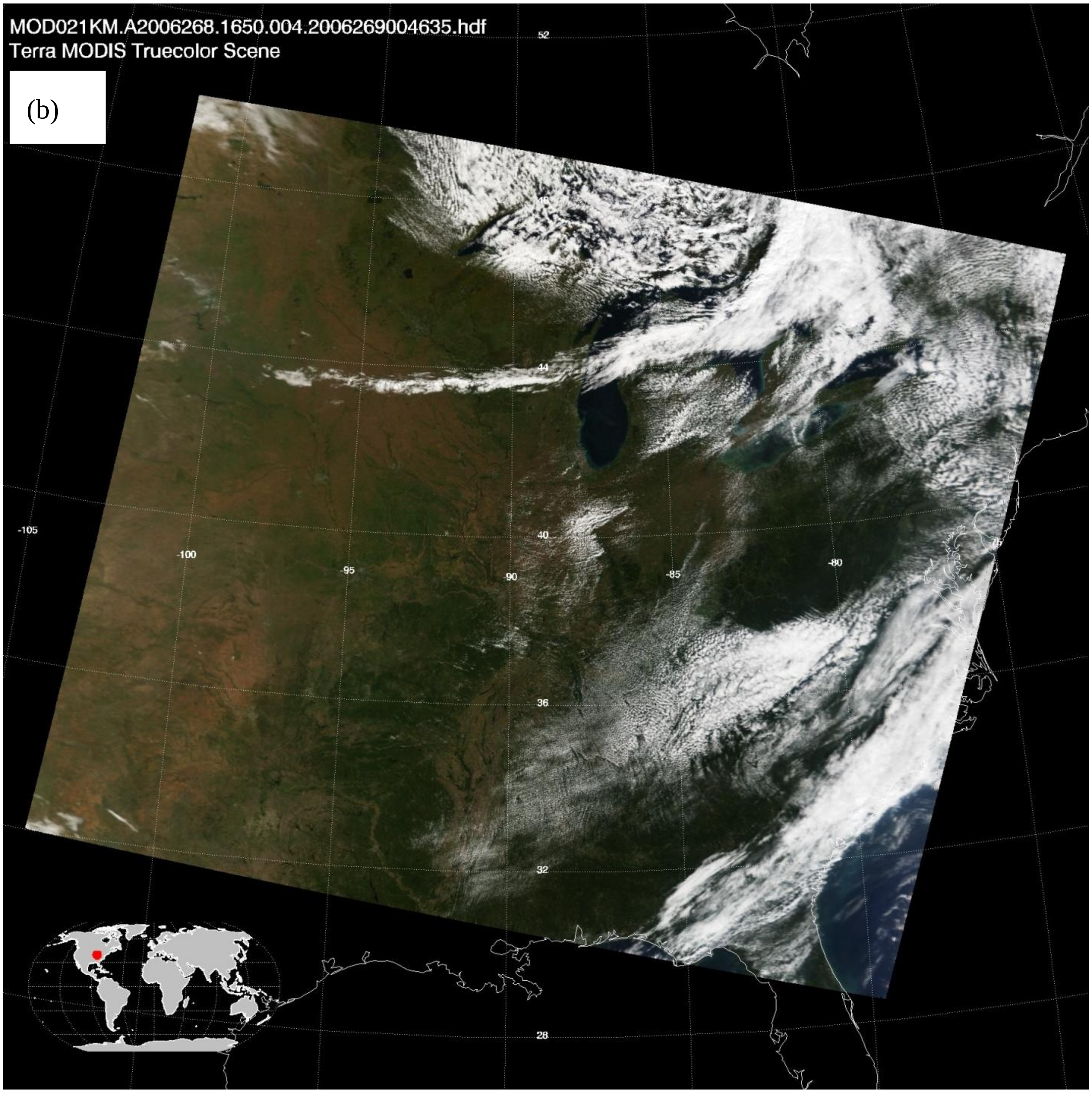
MOD021KM.A2006268.1650.004.2006269004635.hdf
Terra MODIS Truecolor Scene
(b)
52
44
40
36
32
28
-105
-100
-95
90
-85
-80

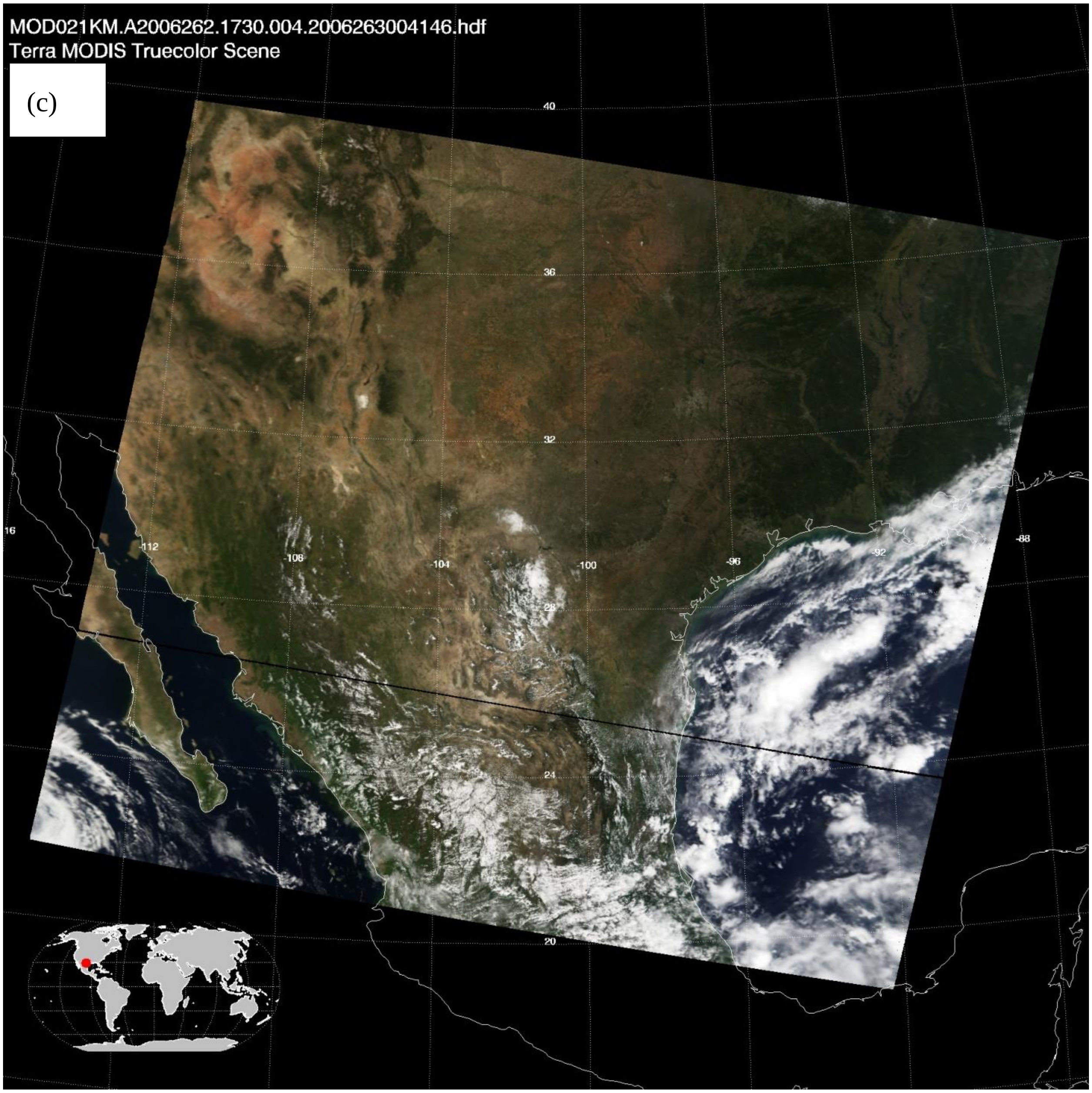

Fig. S9. (a) MODIS true color image (http://modis-atmos.gsfc.nasa.gov/IMAGES/index.html) at 17:00 UTC (local time: 11:00). The black lines indicate the trajectory of the WP-3 path. The WP-3 flew in the early afternoon hours through northeastern Texas covered by sparse clouds. (b) MODIS true color image at 16:50 UTC (local time: 10:50) on September 25; over most areas of Texas, it was clear sky and cloud-free. (c) MODIS true color image at 17:30 UTC (local time: 11:30) on September 19; over most areas of Texas, it was clear sky and cloud-free.

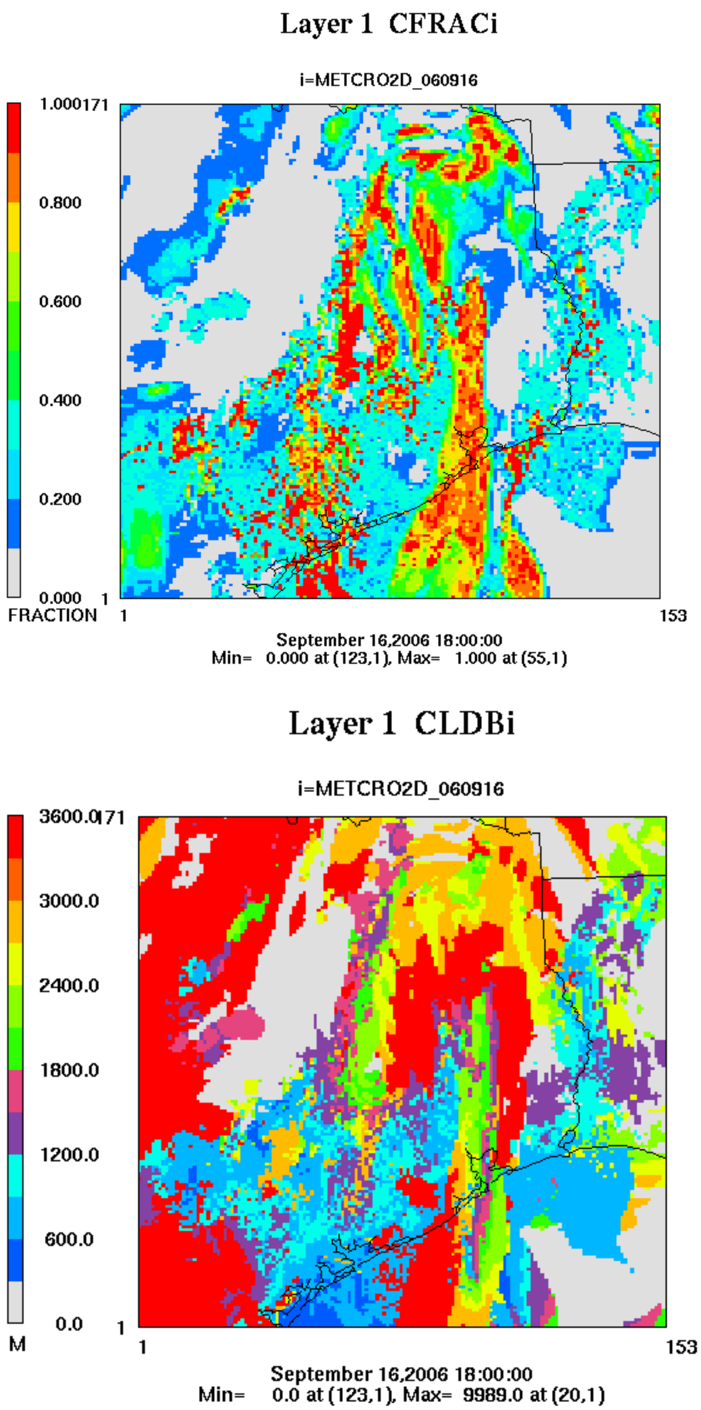

Fig. S10. Modeled (a) cloud cover fraction and (b) cloud bottom height over Texas on September 16, 2006 (18:00 UTC, local time 12:00).

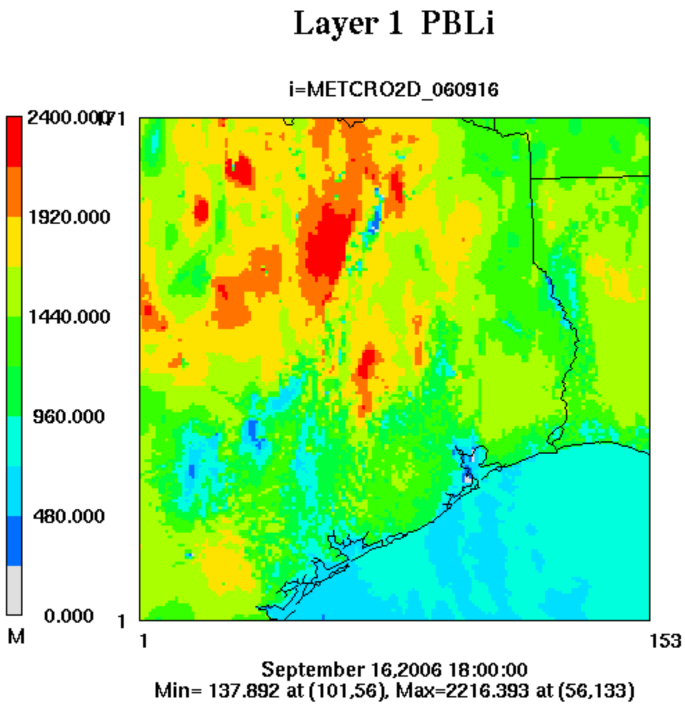

Fig. S11. Modeled planetary boundary layer height at 18:00 UTC (local time: 12:00)

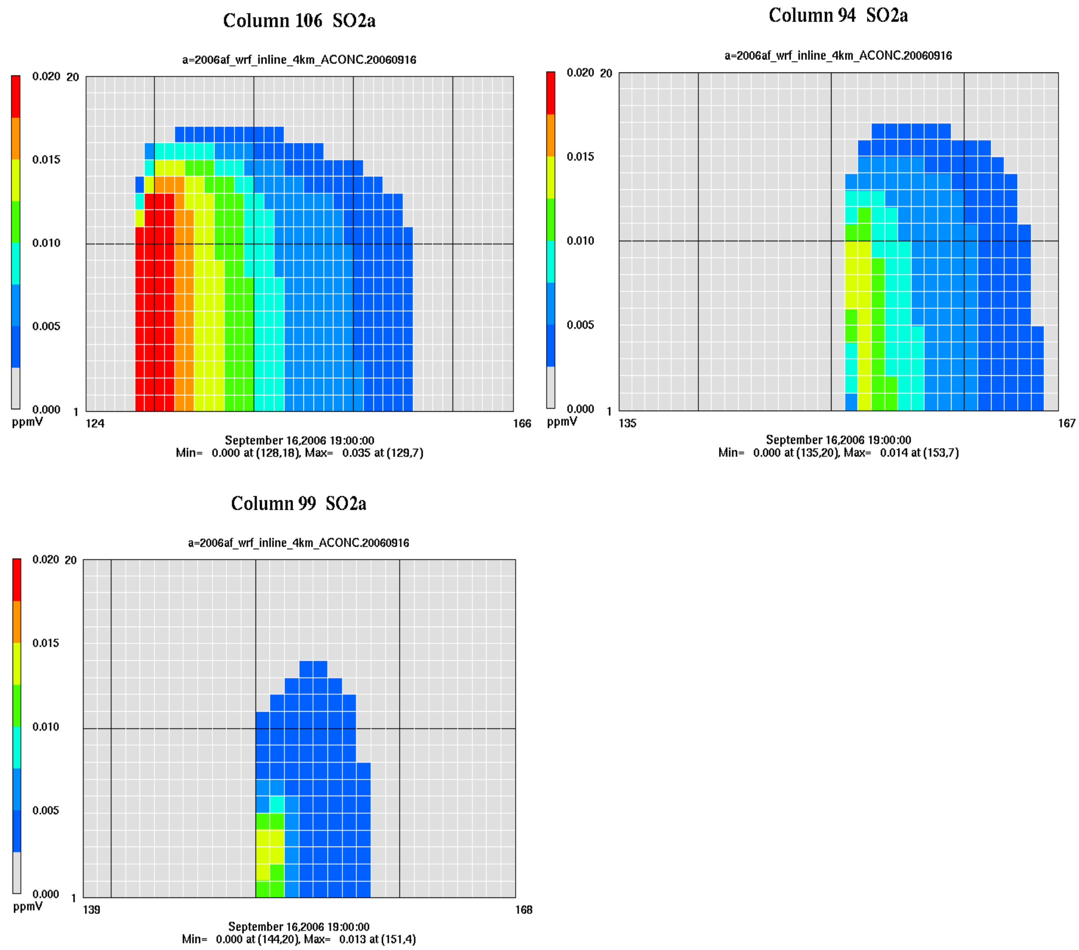

Fig. S12. Vertical distribution (SO_2 concentration in ppm unit) of Martin Lake (a), Monticello (b), and Welsh plumes (c) on September 16. Vertical axis is the model layers.

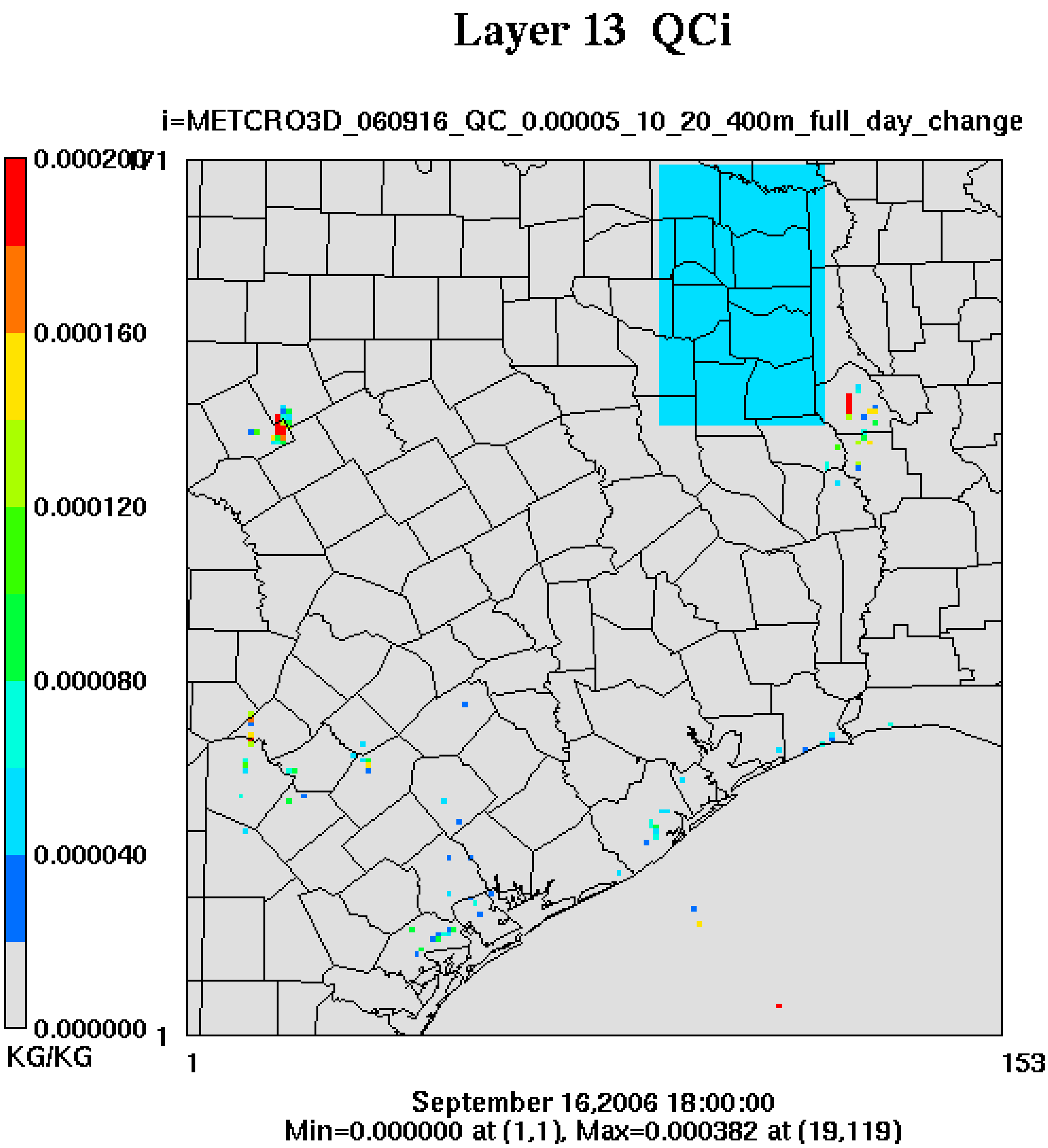

Fig. S13. The region (light blue) for adjusting the cloud liquid water mixing ratio (QC, KG/KG) in the modeling domain. In the northeastern Texas, QC is uniformly set to 0.00005 KG/KG, 0.0005 KG/KG, and 0.005 KG/KG. Layer 13 corresponds to about 1000 m.

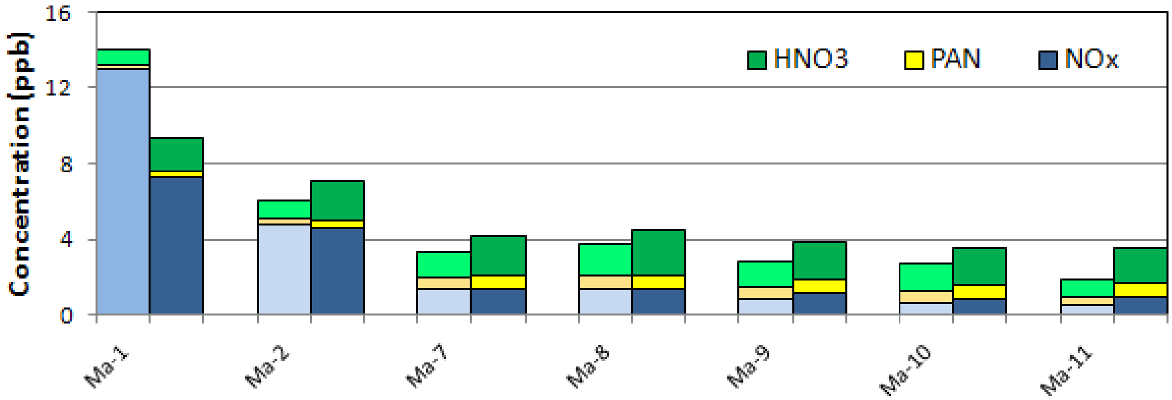

Fig. S14. Concentrations of HNO_3 (green), NO_x (blue), and PAN (yellow) at Martin Lake plume transects from observation (left bars with light colors) and model (right bars with dark colors); one of NO_x, HNO_3, or PAN was not measured at Ma-3, Ma-6, and Ma-12. The observed and modeled concentrations are the average at transects.

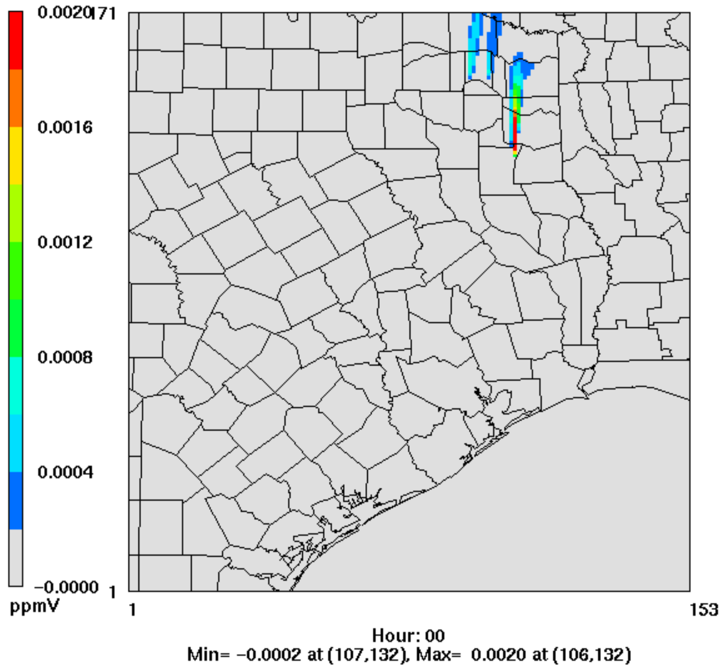

Fig. S15. Difference of ZOC(SO_2) for Martin Lake, Monticello, and Welsh plumes at layer 10 between the base case and QC_0.05 averaged over 17:00 to 20:00 UTC.

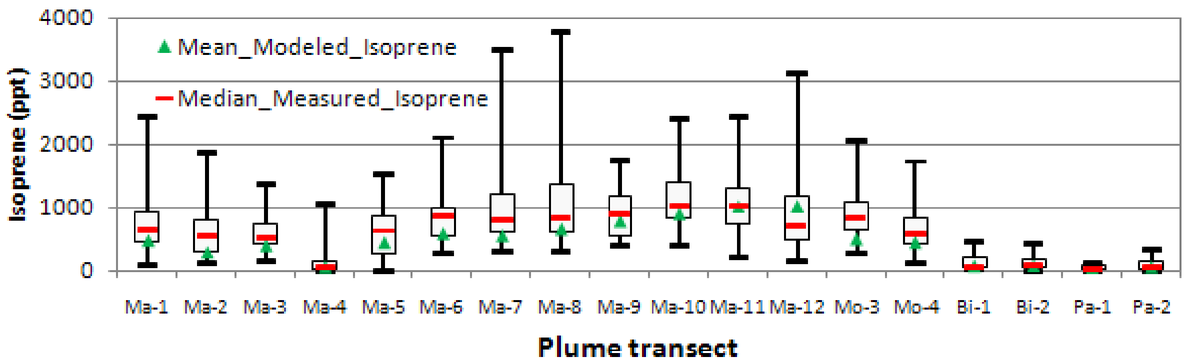

Fig. S16. Modeled (green triangle) and observed (box-and-whiskers) concentration at all transects on 16 and 25 September. The boxes show 25th and 75th percentiles of observations; red lines show medians, and whiskers show minimum and maximum values.

Table S1 Model layer height

Layer	Height(m)
1	43
2	86
3	129
4	172
5	260
6	349
7	436
8	525
9	616
10	706
11	798
12	888
13	1074
14	1266
15	1455
16	1650
17	1851
18	2157
19	2477
20	2904
21	3477
22	4081
23	4994
24	5064
25	6384
26	7165
27	8017
28	8950
29	9981
30	11030
31	12580
32	13441
33	15439
34	18328

Table S2. Instruments and time resolution of major gas-phase species discussed

Species	Reference	Instrument	Time resolution of measurement (second)
O_3	Ryerson et al., 1998	NO-induced Chemiluminescence (CL)	1
NO	Ryerson et al., 1999	O_3-induced CL	1
NO_2	Ryerson et al., 2000	UV photolysis CL	1
HNO_3	Neuman et al., 2000	SiF_5^- Chemical Ionization Mass Spectrometry (CIMS)	1
NO_y	Ryerson et al., 1999	Au converter CL	1
SO_2	Ryerson et al., 1998	Pulsed UV fluorescence	1
CO	Holloway et al., 2000	VUV resonance fluorescence	1
CO_2	Peischl et al., 2010	NDIR absorption	1
Isoprene	de Gouw et al., 2003	Proton Transfer Reaction Mass Spectrometry (PTRMS)	17
PAN	Slusher et al., 2004	CIMS	2

Table S3. Plume transects measured on 16, 19 and 25 September

Facility	Transect [a]	Distance from plant (km)	Flight height (m)	Average wind speed (m/s)	Plume age [b] (hours)
Martin Lake	Ma-1	17.3	660	7.4	0.7
Martin Lake	Ma-2	27.0	660	6.1	1.1
Martin Lake	Ma-3	37.1	660	7.1	1.5
Martin Lake	Ma-4	52.6	1800	8.8	2.0
Martin Lake	Ma-5	52.6	1080	7.9	2.0
Martin Lake	Ma-6	52.6	640	5.4	2.0
Martin Lake	Ma-7	52.6	490	6.8	2.0
Martin Lake	Ma-8	52.6	300	5.5	2.0
Martin Lake	Ma-9	67.5	660	2.9	3.4
Martin Lake	Ma-10	88.1	640	4.0	4.8
Martin Lake	Ma-11	105.7	650	4.7	5.9
Martin Lake	Ma-12	115.9	650	4.2	6.6
Monticello	Mo-1	7.8	640	8.0	0.3
Monticello	Mo-2	27.7	650	6.3	1.2
Monticello	Mo-3	47.9	650	8.1	1.6
Monticello	Mo-4	67.7	660	7.8	2.4
Welsh	We-1	11.5	640	8.4	0.4
Welsh	We-2	31.6	650	5.7	1.4
Welsh	We-3	51.7	650	8.9	2.0
Welsh	We-4	71.8	660	8.0	2.5
Big Brown	Bi-1	20.3	630	4.2	1.3
Big Brown/Limestone	Bi-2	95.7	624	6.4	3.3
Parish	Pa-1	13.5	476	5.9	0.6
Parish	Pa-2	43.3	482	7.0	1.2
Parish	Pa-19-1	3.2	471	4.1	1.5
Parish	Pa-19-2	10.0	491	5.4	4.9
Parish	Pa-19-3	12.3	462	5.0	6.1
Parish	Pa-19-4	14.5	476	5.9	6.9

Parish	Pa-19-5	20.6	488	6.2	10.6

[a] the downwind locations of the plume transects listed in this table are marked in Fig. 2 and Fig. S5 and S6 in supplement

[b] plume age is computed as the distance of plume transect from plant divided by the measured average wind speed at plume transect

Table S4. Background and plume O_3 (ppb) and OPE (unitless) from model and observations.

transect	OBS_O$_3$_BG[a]	MOD_O$_3$_BG[b]	OBS_ΔO_3[c]	MOD_ ΔO_3[d]	OBS_OPE[e]	MOD_OPE[f]
Ma-1	30.0	46.5	-2.6	-0.6	-	-0.5
Ma-2	34.0	49.6	-1.0	1.5	-	1.9
Ma-3	37.3	47.0	2.4	2.0	2.6(0.30)	2.5
Ma-6	34.0	51.5	8.9	8.0	7.2(0.90)	4.7
Ma-7	34.9	52.1	-	8.4	6.2(0.69)	4.0
Ma-8	35.5	52.9	-	8.3	6.8(0.94)	4.3
Ma-9	37.4	51.3	9.7	9.5	6.7(0.80)	5.5
Ma-10	38.3	50.3	8.9	7.0	8.7(0.96)	4.9
Ma-11	37.0	44.2	7.9	5.2	10.1(0.93)	4.9
Ma-12	37.0	45.4	7.4	5.3	-	5.1
Mo-1	32.7	44.3	-1.8	-0.6	-	-1.0
Mo-2	35.1	47.6	2.0	1.3	1.4(0.30)	4.1
Mo-3	37.0	49.3	4.8	4.0	8.3(0.90)	5.5
Mo-4	36.2	48.1	4.5	2.4	10.4(0.94)	4.9
We-1	32.7	44.3	-1.2	-1.1	-	-1.9
We-2	35.1	47.6	4.8	2.8	4.6(0.79)	4.1
We-3	37.0	49.3	5.3	4.0	9.4(0.71)	4.4
We-4	36.2	48.1	7.4	5.2	10.7(0.75)	4.6
Bi-1	-	44.2	-	3.1	1.7 (0.75)	1.5
Bi-2	-	46.3	-	2.0	-	2.9
Pa-1	-	52.4	-	-1.3	4.4(0.41)	-6.5
Pa-2	-	53.5	-	0.4	4.0(0.83)	1.0

[a] OBS_O$_3$_BG: observed background O_3 (in parentheses, dashes mean no valid value can be found for OBS_O$_3$_BG)

[b] MOD_O$_3$_BG: modeled background O_3

[c] OBS_ ΔO_3: OBS_O$_3$_Plume - OBS_O$_3$_BG (in parentheses, dashes mean no valid value can be found for OBS_ΔO_3_BG)

[d] MOD_ ΔO_3: ZOC_{O3} (=$O_{3\ \text{model, base}} - O_{3\ \text{model, zero-out that plant}}$)

[e] OBS_OPE: ozone production efficiency of observed plume from the least square fits of O_3 to (NO_y-NO_x); values in parentheses are the R^2 of least square fit of O_3 to (NO_y-NO_x) (in parentheses, dashes mean no valid value can be found for OBS_OPE)

[f] MOD_OPE: ozone production efficiency of modeled plume (=$ZOCo_3/ZOC_{NOz}$)

References

de Gouw, J., Warneke, C., Karl, T., Eerdekens, G., van der Veen, C., and Fall, R.: Sensitivity and specificity of atmospheric trace gas detection by proton-transfer-reaction mass spectrometry, International Journal of Mass Spectrometry, 223-224, 365-382, 2003.

Holloway, J. S., Jakoubek, R. O., Parrish, D. D., Gerbig, C., Volz-Thomas, A., Schmitgen, S., Fried, A., Wert, B., Henry, B., and Drummond, J. R.: Airborne intercomparison of vacuum ultraviolet fluorescence and tunable diode laser absorption measurements of tropospheric carbon monoxide, J. Geophys. Res. - Atmos., 105, 24251-24261, 10.1029/2000jd900237, 2000.

Neuman, J. A., Gao, R. S., Schein, M. E., Ciciora, S. J., Holecek, J. C., Thompson, T. L., Winkler, R. H., McLaughlin, R. J., Northway, M. J., Richard, E. C., and Fahey, D. W.: A fast-response chemical ionization mass spectrometer for in situ measurements of HNO[sub 3] in the upper troposphere and lower stratosphere, Rev. Sci. Instrum., 71, 3886-3894, 2000.

Peischl, J., Ryerson, T. B., Holloway, J. S., Parrish, D. D., Trainer, M., Frost, G. J., Aikin, K. C., Brown, S. S., Dubé, W. P., Stark, H., and Fehsenfeld, F. C.: A top-down analysis of emissions from selected Texas power plants during TexAQS 2000 and 2006, J. Geophys. Res. - Atmos., 115, D16303, 10.1029/2009jd013527, 2010.

Ryerson, T. B., Huey, L. G., Knapp, K., Neuman, J. A., Parrish, D. D., Sueper, D. T., and Fehsenfeld, F. C.: Design and initial characterization of an inlet for gas-phase NOy measurements from aircraft, J. Geophys. Res. - Atmos., 104, 5483-5492, 10.1029/1998jd100087, 1999.

Ryerson, T. B., Williams, E. J., and Fehsenfeld, F. C.: An efficient photolysis system for fast-response NO2 measurements, J. Geophys. Res. - Atmos., 105, 26447-26461, 10.1029/2000jd900389, 2000.

Slusher, D. L., Huey, L. G., Tanner, D. J., Flocke, F. M., and Roberts, J. M.: A thermal dissociation chemical ionization mass spectrometry (TD-CIMS) technique for the simultaneous measurement of peroxyacyl nitrates and dinitrogen pentoxide, J. Geophys. Res. - Atmos., 109, D19315, 10.1029/2004jd004670, 2004.